2018

EFFECTS OF GLI-SIMILAR 3 KNOCKOUT MUTATIONS ON THE EXPRESSION OF INSULIN TRANSCRIPTION AND PANCREATIC ISLET DEVELOPMENT IN ZEBRAFISH

Dylan James Hammrich
Murray State University

Follow this and additional works at: https://digitalcommons.murraystate.edu/etd

Part of the Biology Commons, Genetics Commons, and the Molecular Genetics Commons

EFFECTS OF GLI-SIMILAR 3 KNOCKOUT MUTATIONS ON THE EXPRESSION OF INSULIN TRANSCRIPTION AND PANCREATIC ISLET DEVELOPMENT IN ZEBRAFISH

A thesis
Presented to
The Faculty of the Department of Biological Sciences
Murray State University
Murray, Kentucky

In Partial Fulfillment
of the Requirements for the Degree
of Master of Science in Biology

By Dylan Hammrich
May 2017

Acknowledgements

There are many people who I would like to thank for putting so much time and effort into helping me complete this project. My thesis advisor, Dr. Gary Zeruth, has been an irreplaceable asset. His endless support through troubleshooting, reworking project ideas, and mercilessly critiquing my writing has allowed me to grow as a biomedical researcher. I would also like to take the time to thank my committee members, Dr. Alexey Arkov, Dr. David Canning, Dr. J. Ricky Cox, and Dr. Chris Trzepacz for dedicating the time necessary for me to complete my project, and for having faith that I was capable of finishing on time. Additionally, I am thankful to the Murray State Department of Biological Sciences for the opportunities that have been provided me.

My research would not have been completed were it not for the support of the fellow ZeRuth lab researchers Tyler Hoard, Katie Alexander, Erin Clayton, and Lilyanne Grieve. Having stories of Tyler's previous graduate experience to laugh about when my own experiments were not running accordingly was its own source of comfort. The help (and more often than not, distractions) provided by the undergrad students allowed me to keep from being too overly focused and losing my mind to the endless hours of writing.

The end result of this work would have been virtually impossible without the loving support of my wife, Lakin Hammrich, without whom I would have never even made it into the graduate program. Her endless support, and willingness to practically raise our kids alone while I spent endless hours doing research, writing this thesis, and going to conferences has given me the drive to do everything necessary to make this all worthwhile. This journey would not have been a success without her.

Abstract

Blood glucose homeostasis is a critical component in the physiological health of vertebrates. Regulation of blood glucose levels is the responsibility of the endocrine pancreas, which excretes hormones to the bloodstream in response to changes in glucose concentrations. The hormones excreted from the pancreas include insulin, which is secreted form the β cells of the pancreas and signals uptake of excess glucose by the peripheral tissues, and glucagon, which is secreted from the α cells and signals release of glucose to the bloodstream through gluconeogenesis in the liver. The Krüppel-like zinc finger protein Gli-Similar 3 (Glis3) is a transcription factor that has been shown to play a critical role in the development of β cells and transcription of the insulin gene.

Defects in the secretion and production of insulin are associated with the development metabolic diseases such as diabetes *mellitus*. Using genome wide association studies, GLIS3 has been identified as a risk locus for the development of both type 1 and type 2 diabetes *mellitus* and neonatal diabetes and hypothyroidism (NDH). Mice with ubiquitous knockouts of Glis3 exhibit phenotypes similar to that of humans, but conditional knockouts specific to the pancreas have produced mice with less severe phenotypes, leaving the role of Glis3 largely enigmatic.

The zebrafish (*Danio rerio*) has emerged as a powerful organism in studying pancreatic development due to its rapid development, short generation time, and transparent, externally developing embryos. The zebrafish pancreas is both morphologically and functionally comparable to that of humans, and the developmental programs that are responsible for pancreatic development appear to be highly conserved

between the two. Zebrafish also have the unique ability to regenerate their β cells after complete ablation without the need for insulin treatment. These factors have made zebrafish a powerful model for the study of pancreatic development and diabetes.

We found that expression of glis3 mRNA begins after 14.5 hours post fertilization (hpf) in zebrafish. Zebrafish pancreas formation begins at approximately 24hpf, but whole mount *in situ* hybridization data shows that glis3 expression is restricted to the zebrafish brain until approximately 48hpf, when expression can be visualized in the pancreas. During this time frame glis3 expression levels increase, which coincide with the visualization of glis3 in the zebrafish pancreata.

Finally, we found that reduction of glis3 through a knockout mutation led to increased production of insulin and glucagon mRNA. Additionally, glis3 heterozygous mutants exhibited a heightened ability to control blood glucose levels, with less variability of blood glucose levels between individuals under fasting, postprandial, and high fat diet conditions when compared to wildtype fish. After four months exposure to a high fat, high glucose diet, wildtype zebrafish expressed heightened levels of resting blood glucose, while heterozygous mutants showed no increase in blood glucose levels when compared to a normal diet.

Collectively, the results of this project provide novel information regarding the regulation of insulin in glis3 mutant zebrafish. A decrease in glis3 expression levels may increase the propensity for an organism to begin the compensatory mechanism for β cell mass expansion, giving insight into possible models for clinical therapies for the treatment of diabetes.

Table of Contents

List of Figures

List of Tables

Introduction

The Pancreas

The pancreas is a complex glandular organ located in the gut cavity that has multiple functions in vertebrate physiology. The pancreas is comprised of three distinct cell populations, including the acinar or exocrine cells, the pancreatic ductal cells, and the endocrine cells. These distinct cell populations give rise to the multiple functions of the pancreas. The acinar cells are responsible for the excretion of enzymes into the lumen of the small intestine, where they play a major role in the digestion of nutrients (Williams 2010). The ductal cells form the pancreatic duct, or duct of Wirsung, and connect the pancreas to the common bile duct and arise from the same bipotent trunk progenitor cells as the endocrine cells (Alpert et al. 1988, Solar et al. 2009). The endocrine cells of the pancreas are responsible for the excretion of hormones into the bloodstream, which play a role in maintaining blood glucose homeostasis. The endocrine cells provide approximately only 4% of the cell population of the pancreas in mice but are composed of a variety of cell types including α cells, β cells, Ɛ cells, δ cells, and pancreatic polypeptide (PP) cells (Pelletier 1977, Andralojc et al. 2009). Each endocrine cell type is primarily responsible for the excretion of its own hormone: α cells secrete glucagon, β cells secrete insulin, Ɛ cells secrete ghrelin, δ cells secrete somatostatin, and PP cells secrete pancreatic polypeptide. The endocrine cells of the pancreas are arranged into the islets of Langerhans, spherical clusters that are embedded into the exocrine tissues of the pancreas (Slack 1995). The primary structure of the islet consists of a majority of centrally located β cells with a periphery of α cells, indicating the importance of glucagon

and insulin in islet function (Fig. 1). These islets are closely associated with neurons in order to facilitate rapid response in blood glucose to changes in physiological conditions.
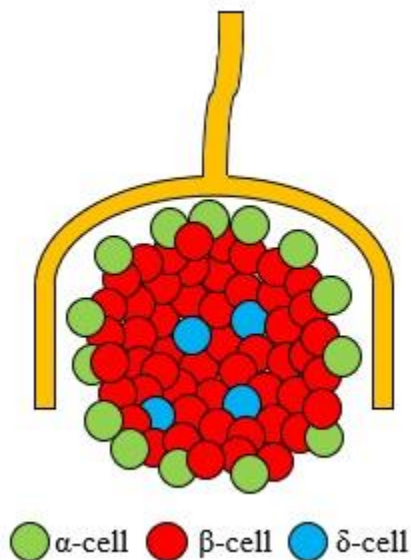
Figure 1. The structure of the primary islets of the pancreas. The central mass of the islet consists primarily of insulin-producing β cells (80% of islet mass) with interspersed δ cells (5% of islet mass). The periphery of the primary islet consists of glucagon producing α cells (20% of islet mass). Axons from nearby neurons surround islets to signal physiological conditions.

Organogenesis of the pancreas is a complex series of steps mediated by a number of transcription factors. Pancreatic endocrine and exocrine cells originate from a population of progenitor cells that arise during the differentiation of the gut endoderm. During the anterior to posterior patterning of the endoderm several transcriptional cues cause the posteriorization of the endoderm, including fibroblast growth factor (FGF) 4 and bone morphogenic protein (BMP) which specify foregut fate. (Deutsch et al. 2001, Rossi et al. 2001, Gu et al. 2002). Retinoic acid (RA) and the Wnt/β-catenin pathway are also required in order to signal the posterior region of the gut endoderm. (McLin et al. 2007, Bayha et al. 2009). This anterior-posterior patterning of the gut endoderm gives rise to two separate epithelial buds on opposing sides of the foregut endoderm; one dorsally and one ventrally. These buds elongate alongside the prospective duodenum and

stomach and fuse together into a single organ as the gut endoderm rotates (Pictet et al. 1972).

Due to the formation of the pancreas as two convergent buds, the dorsal-ventral patterning that gives rise to these buds is extremely important. The presence of RA is used to signal in part for the dorsal bud formation, but evidence shows that close proximity to the endothelial cells of the fusing aorta is responsible for dorsal patterning (Lammert et al. 2001). Before the fusion of the dorsal aorta the presumptive dorsal bud of the pancreas is proximal to the notochord while it secretes activin-β and FGF 2, which suppress Sonic hedgehog (Shh) and lead to early dorsal patterning (Hebrok et al. 1998).

Proximity of the gut endoderm to the vitelline veins and lateral plate mesoderm (LPM) before fusion of the buds begins ventral patterning (Spooner et al. 1970, Lammert et al. 2001). Though less is known about the included pathways, signaling for the ventral pancreatic bud appears to be closely related to that of the dorsal bud. Dependence on external signals including activin-β, BMP, and RA seems to remain the same, though signals from the cardiac mesoderm which signal for dorsal development must be blocked (Lammert et al. 2001, Rossi et al. 2001). Expression of transformation growth factor (TGF) β has been shown to play an important role in blocking these dorsal patterning signals and leads to formation of the ventral bud (Wandozioch and Zaret 2009). Absence of FGFs and cardiogenic mesenchyme during development of the dorsal bud will lead to the formation of a second ventral bud, indicating that this may be the "default," and additional signals are needed to cause the formation of the dorsal bud (Deutsch et al. 2001).

After the signal induction from the notochord and LPM rapid cellular proliferation will give rise to the forming dorsal and ventral buds, respectively. Pancreatic endocrine cells arise from the dorsal bud, which begin to form the primary islets of α and β cells. The ventral bud is responsible for formation of the acinar and ductal cells. As development continues the gut endoderm rotates and brings these two buds together where they begin to fuse (Golosow and Grobstein 1962). After fusion, the ventral bud of the pancreas will begin rapid proliferation of cells as branches begin to form. These branches will form the ducts used to transport digestive enzymes in the gut. The leading cells in these expanding branches excrete pancreatic transcription factor 1 (Ptf1a) and will give rise to the acinar cells after the enzymatic ducts form (Zeechin et al. 2003). Bipotent trunk progenitors follow the leading Ptf1a expressing tip cells, which are capable of forming both ductal and endocrine cells during the secondary transition, a developmental stage where pancreatic progenitor cells are rapidly and terminally differentiated into their final cell fates (Wang et al. 2005, Zhou et al. 2007).
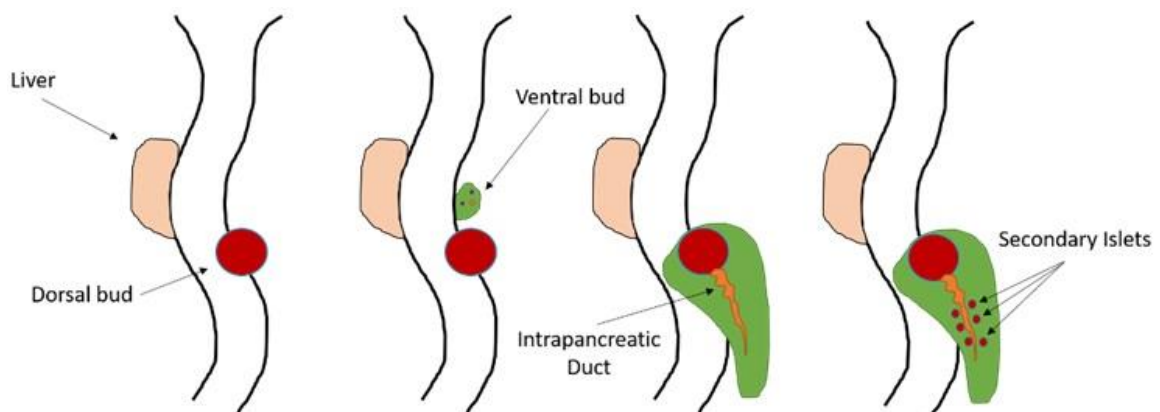
Figure 2. Formation of the pancreas from convergent buds in rodents. Signals from the notochord induce the dorsal bud, which gives rise to the α and β cells. Signals from the lateral plate mesoderm cause induction of the ventral bud, which gives rise to the acinar and ductal cells. Twisting of the gut endoderm causes the fusion of the dorsal and ventral bud. Rapid proliferation and branching of pancreatic progenitor cells form the pancreatic ducts and the secondary islets emerge.

Blood Glucose Homeostasis

In the mature organism, production and secretion of hormones from the α and β cells of the primary islets is highly regulated in order to maintain normal blood glucose levels. This rapid response system is imperative in maintaining a healthy physiological state. Insulin is expressed in response to high glucose levels when ATP generated during oxidative respiration depolarizes the plasma membrane. Ca^{++} ion channels open when the plasma membrane is depolarized, leading to the secretion of insulin (Braun et al. 2008). This secreted insulin then signals peripheral tissues to absorb glucose to use as energy or adipose tissue to convert glucose into fat for sorage, leading to decreased blood glucose levels. When blood sugar levels decrease insulin is down regulated, and glucagon is secreted from the α cells of the primary islets into the bloodstream. This glucagon is absorbed by the liver stimulating gluconeogenesis. Glucose created during this process is released into the blood stream in order to normalize blood glucose levels.
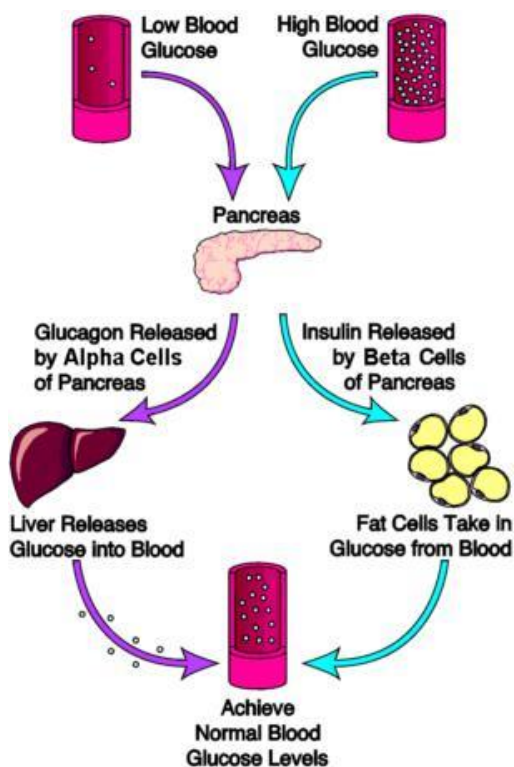
Figure 3. Schematic of pancreatic blood glucose homeostasis. At times of high blood glucose, insulin is released from β cells of the pancreas. Insulin signals periphery and adipose tissues to absorb glucose for energy and conversion into fat, decreasing blood glucose levels. At times of low blood glucose, α cells of the pancreas secrete glucagon, signaling for the liver to begin gluconeogenesis. This process forms glucose from fat, which is released to increase blood glucose levels.

Following a marked increase in blood glucose levels, ubiquitous and β cell specific activators bind to the 340 base pair (bp) promotor region located upstream of the insulin transcription start site (Ohneda et al. 2000, Melloul et al. 2002). The transcription factors pancreatic and duodenal homeobox-1 (Pdx 1), V-maf musculoaponeurotic fibrosarcoma oncogene homologue A (MafA) and neurogenic differentiation 1 (NeuroD1) are among the transcription factors responsible for the expression of insulin in response to glucose levels in β cells (Armata et al. 2007, Kaneto et al. 2007, Kataoka 2007). As insulin is transcribed, it is stored in secretory vesicles in the cytoplasm to replenish insulin levels after secretion. In times of low blood glucose, the transcription factors responsible for the expression of insulin are down regulated through multiple mechanisms. Pdx 1 is controlled through a phosphorylation dependent manner which prevents its interaction with co-activators during times of low blood glucose (Mosley and Ozcan 2004). NeuroD1 localization is affected by glucose levels, and at low concentrations is located cystolicly, preventing its interaction with the insulin promoter region (Marcus et al. 1998). MafA is the insulin transcription factor most tightly controlled by glucose levels, and is only transcribed when cellular glucose levels rise above 10-25 mM concentrations (Sharma and Stein 1994).

Diabetes *mellitus* is characterized by β cell dysfunction and the inability to regulate blood glucose. Neonatal diabetes mellitus (NDM) and mature-onset diabetes of the young (MODY) are both monogenic forms of diabetes that affect children (Hattersley et al. 2009). In these forms of diabetes, a single gene mutation reduces the body's ability to express insulin. Type 1 diabetes *mellitus* (T1DM) is caused the inability of the pancreas to express insulin, due to an autoimmune-mediated destruction of β cells

(Goodison et al. 1992). In type 2 diabetes *mellitus* (T2DM), tissues peripheral to the pancreas become resistant to insulin, decreasing the efficiency of the body to regulate blood glucose levels (Taniguchi et al. 2006). Along with this, it has been shown that insulin resistance can be compounded by deteriorating function of β cells and decreased islet mass (Talchai et al. 2009). The molecular mechanisms underlying the development T1DM and T2DM are currently unclear. Both T1DM and T2DM have been associated with the development of multiple comorbidities, including heart disease, neuropathy, strokes, and kidney failure. The cost of treating the chronic symptoms of diabetes have steadily risen over the years, reaching as high as 245 billion dollars in the US alone in 2012 (Yang et al. 2013a).

Beta Cell Mass Expansion, Neogenesis

Understanding β cell mass regulation is a critical issue in determine the cause of T2DM. Formation of β cells in the primary islets of the dorsal bud from endocrine progenitor cells marks the beginning of insulin transcription and of blood glucose regulation in developing embryos (Rossi et al. 2001, Andralojc et al. 2009). As described above, this initial β cell population arises from the presumptive dorsal bud of the pancreas due to signals from the notochord and endothelial cells of the dorsal aorta. The secretion of FGF from the notochord drives the rapid proliferation of progenitor cells, giving rise to the presumptive islets by signaling for α and β cell fates (Elghazi et al. 2002). During the late gestational period of development, the population of β cells in the pancreas nearly doubles daily. This neogenesis from undifferentiated progenitor cells is assisted by the mitotic activity of the existing β cells, though only about 10% of the already existing β cells are in the mitotic state at any one time (Swenne 1982, Hellerstrom

and Swenne 1991). Neogenesis is the most rapid increase in β cell mass, and this time of

fetal growth seems to be critical for determining the number of β cells in the adult

pancreas. Despite the fact that β cell mass continues to expand after birth, embryos with

severely decreased β cell mass during the late gestational period never catch up to their

healthy counterparts and are more likely to develop glucose intolerance and diabetes

mellitus (Simmons et al. 2001).

In mice, β cells mass expands through neogenesis from ductal cells surrounding

the islet cells for approximately one week. After this time, the precursors that are

responsible for neogenesis of β cells disappear (Bouwens et al. 1994, Solar et al. 2009).

The generation of new β cells then becomes possible only through the mitotic

proliferation of existing β cells, which occurs at a highly decreased rate when compared

to late fetal growth (McEvoy and Madison 1980, Kaung 1994). In models where β cell

proliferation was restricted during the late gestational period through genetic

manipulation or through dietary restriction in the mother, it has been shown that mitotic

proliferation of the existing β cell population is unable to compensate for the loss of the

critical mass expansion from progenitor cells (Garofano et al. 1998, Simmons et al.

2001).

Beta Cell Mass Expansion, Compensation

Throughout adult life, β cell mass increases in order to compensate for the

increased body mass of the individual (Montanya et al. 2000). This compensation is

carried out through the same proliferation mechanism as postnatal growth, and because of

this, the number of islets in the adult pancreas remains constant throughout the life cycle

(Dor et al. 2004, Solar et al. 2009). Even though adult proliferation of β cells is relatively

slow, there is evidence of a compensation of β cell mass in response to excessive weight gain leading to obesity. In rodent models for obesity, there was shown to be a compensatory fourfold increase in β cell mass when compared to lean controls (Pick et al. 1998). The mechanisms of this compensatory mass expansion are currently unknown in mammals, as there does not appear to be an increase in β cell proliferation (Montanya et al. 2000), but may include neogenesis, slight increases in proliferation, or hypertrophy (Arystarkhova et al. 2013).

GLIS3

Krüppel-like zinc finger proteins make up one of the largest families of transcription factors, which is separated into subfamilies based on the number of zinc fingers motifs, sequence homology between the motifs, and the presence of certain transactivation domains (Williams et al. 1995, Poncelet et al. 1998). The Gli-similar 1-3 proteins (Glis 1-3) are a subfamily of the Krüppel-like zinc finger proteins similar to the Gli and Zic subfamilies (Kinzler et al. 1988, Lamar et al. 2001, Kim et al. 2003, 2005). The human gene *GLIS3* is mapped to chromosome 9p24.2 and spans 495 kb, coding for a protein that is 90 kDa. *GLIS3* contains nine exons and eight introns, sharing about 80% homology between the human *GLIS3* and the mouse *Glis3* genes (Kim et al. 2003, 2005). Homologs have also been identified in zebrafish (*glis3*, sharing 48-49% homology), as well as gleeful (*gfl*) and lame duck (*lmd*) in *Drosophila* (Duan et al. 2001, Furlong et al. 2001, ZeRuth et al. 2011) The GLIS3 gene reportedly has several possible alternative transcripts, though the physiological function of any proteins generated by these transcripts is currently unknown (Senee et al. 2006).

The human GLIS3 protein contains a series of five Cys_2-His_2 zinc fingers motifs separated by the conserved amino acid sequence of T/SGEKPY/F, a sequence that is shared with the closely related Zic and Gli subfamilies (Agata et al. 1999, Kim et al. 2003). This domain spans from exons 2-4 of the gene and is used to interact with target DNA sequences (Kim 2003). The GLIS3 zinc fingers can bind at the Glis3 consensus sequence of 5'-(G/C)TGGGGGG(A/C)-3' (Beak et al. 2008) and the closely related Gli protein consensus sequence, although with much lower affinity (Lamar et al. 2001, Nakashima et al. 2002, Kim et al. 2003). The GLIS 3 gene also contains a transactivation domain on the C-terminal end that is critical in the activation of target genes (Kim et al. 2003, Beak et al. 2008) as well as an N-terminal conserved region (Fig. 4). The function of the N-terminal conserved region is still mostly unknown, but there is some evidence that it serves a role in protein-protein interaction. (Kim et al. 2003, ZeRuth et al. 2015).
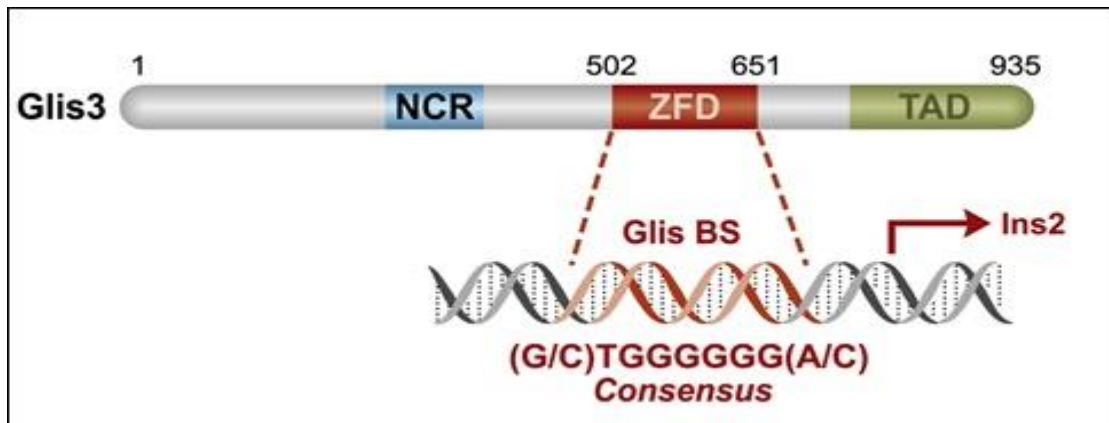
Figure 4. Map of the conserved regions in the Glis3 protein across homologs. Important regions include the N-terminal conserved region (NCR), zinc finger binding domain (ZFD), the C-terminal transactivation domain (TAD), and the Glis binding site (Glis BS). Numbers indicate amino acid positions. (Adapted from Lichti-Kaiser et al. 2012).

Glis3 Localization

During development, Glis3 expression is controlled both temporally and spatially. In mice, Glis3 RNA expression begins at E8.0 and can be seen in the pancreas, kidney, testes, lungs, brain, and eyes (Kim et al. 2003, Kang et al. 2009). Postnatally (E16.5-E18.5) Glis3 expression in the pancreas is restricted to the ductal cells and islet β cells (Senee et al. 2006, Kang et al. 2009). In the adult mouse, Glis3 expression continues in the pancreas, kidney, testes, retinas, brain, and lungs (Kim et al. 2003, Beak et al. 2007). Using EGFP-tagged Glis proteins it has been shown that these proteins are predominately expressed in the nuclei of exponentially growing cells (Kim et al. 2002, 2003, Zhang et al. 2002, Beak et al. 2008). While Glis3 contains nuclear location signals (NLS), mutation of these NLS, along with detailed studies of the mutations of individual zinc fingers (ZF) in the Glis3 ZFD have shown that the NLS are not required for the localization of Glis3 to the nucleus, but that mutation of ZF4 greatly decreases the accumulation of Glis3 in the nucleus (Kim et al. 2003, Zhang et al. 2002, Beak et al. 2008). Along with the nucleus, Glis3 accumulation can be measured in the primary cilium, much like the closely related Gli subfamily of proteins (Haycraft et al. 2005, Hashimoto et al. 2009). The primary cilia of cells are critical for the function of Shh- and Wnt- mediated signaling, and dysfunction of cilia leads to multiple ciliopathies (Oro 2007, Rohatgi et al. 2007, Veland et al. 2009).

Glis3-Associated Pathologies

Because of its early expression during development and the subcellular localization in the nucleus and primary cilia of rapidly proliferating cells, we know that Glis3 plays an important role in developing and adult cells. This is supported by the fact

that disfunction in the expression and transcription of Glis3 in humans has been linked to the development of neonatal diabetes and hypothyroidism (NDH) and polycystic kidney disease (PKD) (Taha et al. 2003, Senee et al. 2006). NDH is characterized by hyperglycemia, hypoinsulemia, neonatal diabetes, and elevated thyroid stimulating hormone (Senee et al. 2006). NDH is also accompanied by multiple severe symptoms, including but not limited to cholestasis, hepatic fibrosis, congenital glaucoma, and facial deformities (Taha et al. 2003, Senee et al. 2006). PKD is characterized by the development of enlarged cysts in the kidneys, leading to kidney failure and death (Taha et al. 2003, Senee et al. 2006).

Glis3 knockout mice exhibit similar phenotypes of Glis3 mutant humans, including NDH, PKD, and small, misshapen primary islets in the pancreas (Kang et al. 2009, Watanabe et al. 2009). One identified target gene for Glis3 is insulin, indicating that Glis3 may play an important role in the development of the endocrine pancreas or in the differentiation of β cells (Kim et al. 2003, Senee et al. 2006, Kang et al. 2009, Yang et al. 2009). This is supported by the fact that a human genome-wide association study has identified GLSI3 as a risk locus for the development of both T1DM and T2DM (Barrett et al. 2009, Boesgaard et al. 2010, Dupuis et al. 2010).

Glis3-Mediated Gene Regulation

The mechanism through which Glis3 dysfunction leads to NDH and PKD are not fully understood, though the localization of Glis3 in the primary cilia gives indication in its role in the development of renal disease. For starters, NDH and PKD are both categorized as ciliopathies, which are caused by disruptions in the primary cilia (Saunier et al. 2005, Bisgrove and Yost 2006, Torres and Harris 2006). The primary cilia are

immotile, thread-like structures that extend from the cell into the extracellular matrix (Bisgrove and Yost 2006, Fliegauf et al. 2007, Berbari et al. 2009). Each cilium is composed of nine microtubule doublets that form an axoneme, surrounded by a continuation of the cellular plasma membrane (Bisgrove and Yost 2006, Berbari et al. 2009). A process called intraflagellular transport (IFT) is used to mediate the travel of ciliary proteins along the length of the axoneme (Rosenbaum and Witman 2002, Fliegauf et al. 2007, Gerdes et al., 2009). Because of the role of IFT in the transport of ciliary proteins into the primary cilia, the primary cilia functions as a chemo-, photo-, and mechano-sensor. The specialized plasmid membrane surrounding the primary cilia also gives it a role in the Shh- and Wnt- dependent signaling pathways (Oro 2007, Rohatgi et al. 2007, Corbit et al. 2008).

Because of the similarities in the Glis and Gli subfamilies of the Krüppel-like zinc finger proteins, it is hypothesized that Glis3 interacts with the primary cilia in a similar mechanism to the Shh/Gli3 pathway (Attanasio et al. 2007, Kang et al. 2009). A hypothetical model of Glis3 activation mirroring that of Gli3, has been suggested due to the similarities in subcellular localization. In this hypothetical model, activation of a membrane bound protein in the cilia activates IFT, leading to accumulation of Glis3 in the primary cilia (Haycraft et al. 2005, Kim et al. 2009, Kang et al. 2010). At this point activation of Glis3 may be dependent on phosphorylation or proteolytic processing. Following this processing and translocation back into the nucleus, Glis3 proteins can then repress or activate the transcription of target genes (Kim et al. 2002, Kang et al. 2009, Kang et al. 2010). More study is needed in order to identify the molecular components for each step, but initial studies have indicated that the Glis3 model appears to be highly

similar to that of the Shh/Gli3 model (Kim et al. 2002, Zhang et al. 2002, Hoskings et al. 2007).

Much like the molecular components of the proposed model for Glis3 activation, the mechanism by which Glis3 activates or repress transcription is not currently known. It has been shown that Glis3 works with multiple cofactors at the site of transcription in order to activate or repress target genes (ZeRuth et al. 2013). Glis3 was shown to be able to recruit Creb-Binding Protein (CBP/p300) (ZeRuth et al. 2013) in order to promote the transcription of insulin through protein-protein interactions with Pdx1, MafA, and NeuroD1 (Naya et al. 1997, Pashavaria et al. 1997, Qiu et al. 1998, Ohneda et al. 2000). Additionally, Glis3 has been shown to interact with WW domain-containing transcriptional regulator 1 (Wwtr1), which in turn interacts with various other transcriptional factors as either a coactivator or corepressor (Hong et al. 2005, Hong and Yaffe 2006, Kang et al. 2009).

Zebrafish as a Model Organism

In recent years, the zebrafish (*Danio rerio*) has begun to emerge as a powerful model for the study of pancreatic development. *Danio* have several advantages over the more commonly used mouse models, including rapid development, short generation time, and an amenability to genetic techniques (Streisinger et al. 1981). A single female can give rise to a clutch of 200-300 transparent, externally developing eggs at a time. The transparency of these eggs is important for the ability to efficiently visualize the developmental processes. Moreover, since zebrafish are reared in water, application of drugs is accomplished by simply placing the drugs in the water, as with tricaine-S anesthesia (Matthews and Varga 2012).

Importantly, the pancreatic development of the zebrafish appears to be highly conserved with that of humans and mice models (Pack et al. 1996, Argenton et al. 1996, 1997). RA signaling in the anterior endoderm specifies for a pancreatic fate, and Wnt/beta-catenin signaling has been shown to be responsible for tissue patterning, much like in mammals (Stafford and Prince 2002, Goessling et al. 2008). The cellular structure of the zebrafish pancreas matches that of mammalian models, with exocrine and ductal cells forming alongside the endocrine cells in two separate buds, one ventral and one dorsal (Argenton et al. 1999, Biemar et al. 2001, Devos et al. 2002, Pauls et al. 2007). Preliminary studies have shown that a fraction replicating β cells persist throughout the life of the adult fish (Yee et al. 2001, Pisharath et al. 2007). This can be related to the replication that is responsible for β cell mass expansion through adulthood in mammals (Kaung 1994, Teta et al. 2005). One unique feature that sets the zebrafish apart from rodent models is that ability to regenerate its β cells after complete ablation (Pisharath et al. 2007, Xu et al. 2008, Moss et al. 2009). The ability of zebrafish to regrow β cells after complete ablation indicates that adult zebrafish have a maintained population of pancreatic progenitor cells, something that seems to be lacking in mammals, as β cell mass expansion appears to be achieved through β cell proliferation alone (Bouwens et al. 1994, Solar et al. 2009). However, in zebrafish β cell mass expansion in response to nutrient excess stems primarily from neogenesis from postmitotic progenitor cells (Enrico et al. 2009). Understanding the mechanisms of β cell mass expansion in response to nutrient excess can be the first step to the development of clinical treatment for β cell dysfunction and glucose intolerance caused by obesity. By understanding the mechanism

through which β cell regeneration is achieved, it is possible that new clinical therapies for T2DM can be explored.

While pancreatic morphology and function appear to be highly conserved between mammals and zebrafish, there are key differences in pancreatic organogenesis. Neurogenin 3, a key transcription factor responsible for the differentiation of islet cells (Gu et al. 2002, Rukstalis and Habener 2009), has no known homologue in zebrafish. Endocrine cell differentiation in zebrafish appears to instead be under control of signaling from the transcription factor Soxb9 (Huang et al. 2016). In addition to this, zebrafish pancreata form endocrine cells in scattered bilateral rows, that migrate to form a single islet during late-somitogenesis (Biemar et al. 2001). Migration of endocrine cells appear to be under the control of glypican knypek (gpc4) as loss of this gene function causes the failure of the bilateral endocrine primordia to merge (Biemar et al. 2001).

Due to a partial duplication of its genome, zebrafish tend to have multiple homologues of genes that are unique in mammals, making complete knockdown studies difficult in some cases (Force et al. 1999, Blader et al. 2004, Zecchin et al. 2007). However, there is only one glis3 ortholog in the zebrafish genome on chromosome 10, which is responsible for encoding a 2,785 bp transcript (Howe et al. 2013, O'Hare et al. 2016). This transcript encodes for a protein that is 787 amino acids and has 49% homology with the human Glis3 gene (Howe et al. 2013). This homology rises to more than 90% when comparing the critical zinc finger binding domains, and luciferase assays have been used to show that zebrafish glis3 is capable if activating the human insulin gene (Howe et al. 2013, ZeRuth et al. 2015).

Preliminary studies of glis3 localization and function have already been performed in zebrafish. Using oligonucleotide riboprobes, glis3 mRNA localization was determined in a process called whole mount *in situ* hybridization. These synthetic riboprobes hybridize to the glis3 transcript sequence and emit a fluorescent signal due to the digoxigenin-11-dUTP used during riboprobe synthesis (Fig. 5A). glis3 expression has been measured in the brain and pancreas of developing zebrafish as early as 24hpf and 48hpf, respectively. Using a process called morpholino knockdown, glis3 RNA translation was blocked using morpholino oligos. This process is becoming an advanced tool for silencing the translation, splicing, or ribosomal activity of target RNAs. By silencing glis3 translation in developing embryos, a marked decrease in the number of insulin and glucagon producing cells is observed (Unpublished data, Fig. 5B).
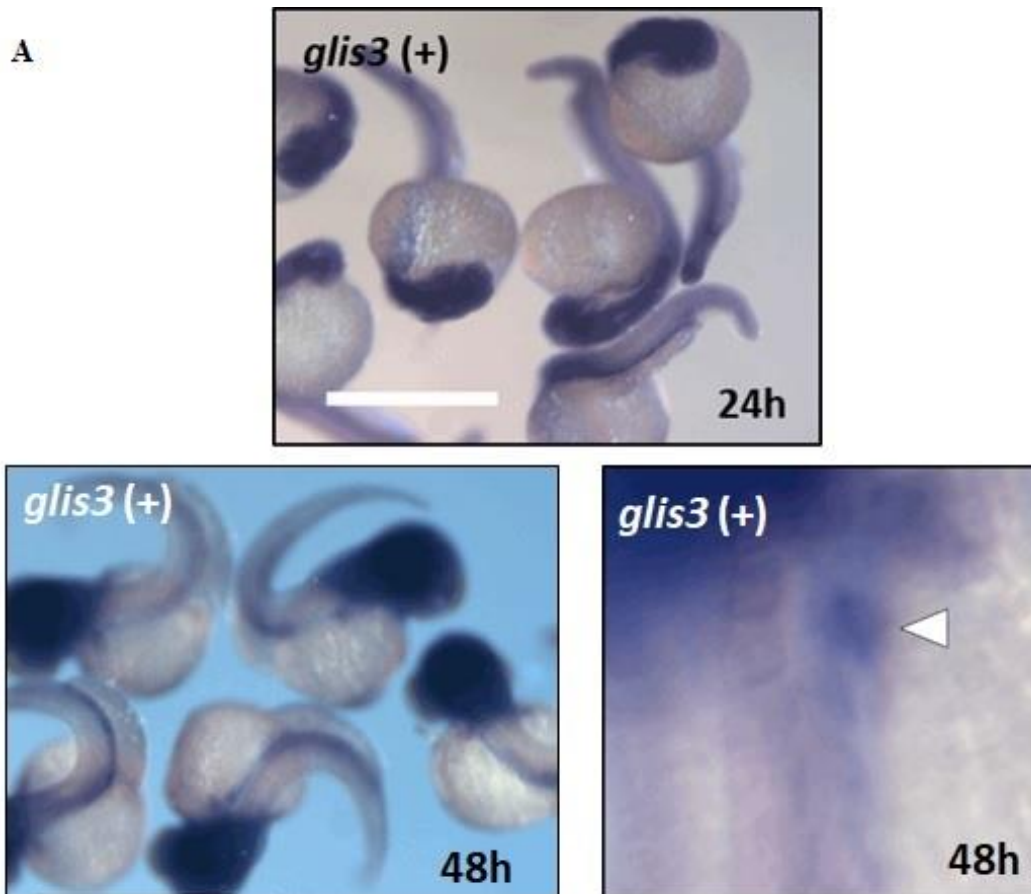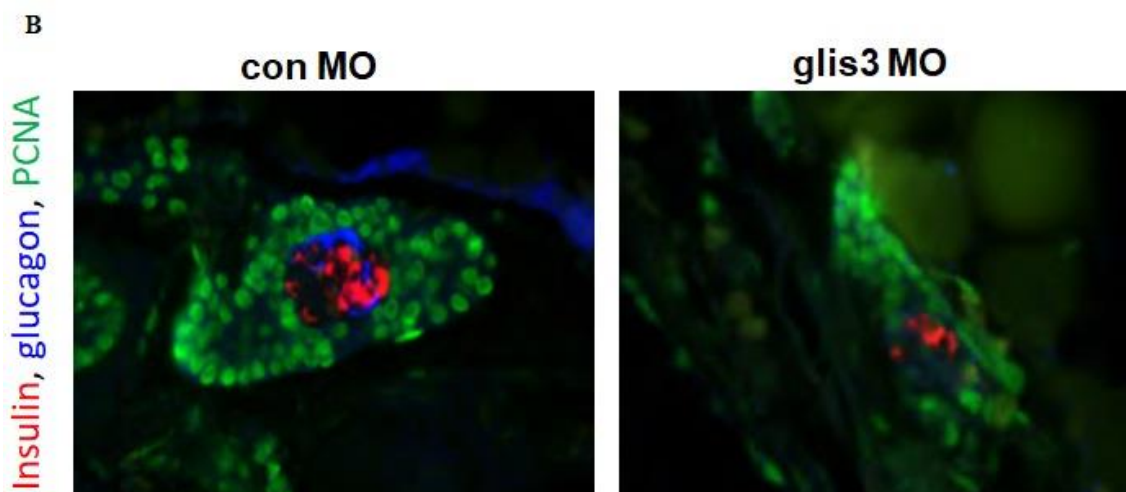
Figure 5. Preliminary analysis of localization and function of glis3. **A.** Whole mount *in situ* hybridization was used to determine the localization of glis3 in developing zebrafish embryos. Fluorescently labeled digoxigenin-11-dUTPs are used to synthesize riboprobes that hybridize to glis3 mRNA. glis3 expression can be seen in the zebrafish brain at 24hpf, and in the developing pancreas as early as 48hpf. **B.** Morpholino oligos were used to silence glis3 mRNA translation. Reduction of glis3 expression due to morpholino knockdown was responsible for a reduction in insulin and glucagon expression in the developing zebrafish pancreas.

Knockout studies of glis3 have been conducted in another small fish model called Medaka (*Oryzias latipes*). A transposon was found to be inserted in the fourth intron of glis3, resulting in a mutated zinc finger binding domain and a truncated protein. Medaka with glis3 nonsense mutation exhibited the expected phenotype of PKD, including renal cyst formation and decreased urine flow rate (Hashimoto et al. 2009). However, unlike humans and mammals Medaka glis3 mutants used showed none of the symptoms of a pancreatic phenotype, indicating a possible redundancy for glis3 in pancreatic function in Medaka (Hashimoto et al. 2009). By using zebrafish as a model organism to study the effects of glis3 mutation, it may be possible to develop models for the study of NDH, T1DM, and T2DM. By subjecting glis3 mutant zebrafish to a high fat, high glucose diet, we hope to identify the effects of glis3 mutations on the pancreatic islet mass expansion in response to nutrient excess. Identification of target genes in pancreatic endocrine cell

differentiation can eventually lead to generation of β cells from induced pluripotent stem cells (iPSCs) for use in β cell transplant. Identification of the mechanisms responsible for regeneration of β cells in zebrafish can lead to the use of regeneration as a clinical therapy in humans for the treatment of type 2 diabetes.

Material and Methods

Zebrafish Housing

The zebrafish where housed using a standard AQUANEERING aquatic housing system. Briefly, adult fish where housed in either 6.0 or 2.8 L tanks, containing a maximum of 30 or 14 fish, respectively (Vargesson 2007). These tanks are part of a five-rack continuous flow system maintained at a pH of 7.0 and a temperature of 27°C. The entire rack system is on a scheduled 14-hour light cycle to optimize zebrafish health and breeding (Lopez-Olmeda et al. 2006). Flowing water undergoes mechano-, UV-, and bio-filtration to remove particulates, microbial life, and ammonia. Half of the water in the system is replaced daily using a timed water exchange tank to supplement the filtration. Zebrafish are fed GEMMA Micro 300 at 5% of biomass once daily.

Zebrafish Lines

The wildtype zebrafish line used is the AB line, ordered from the Zebrafish International Resource Center (ZIRC). The mutant line of zebrafish used is a glis3$^{+/-}$ heterozygote generated by ENU mutagenesis. Generation of mutants through ENU mutagenesis has been previously described (Kettleburough et al. 2013). Specifically, the heterozygous line is glis3$^{+/sa17645}$, and was purchased from ZIRC. This line of mutant fish contains a C/T mutation within exon 2 of the gene coding glis3, resulting in an early stop codon (Fig. 6). This early stop codon leads to a truncated protein containing only 47 amino acids that lacks the zinc finger binding domain, the transactivation domain, and the N-terminal conserved region of glis3. Since it lacks all the conserved regions of glis3 that

have been identified as crucial for glis3 function, it is expected that the protein produced

will act as a sufficient knockout.
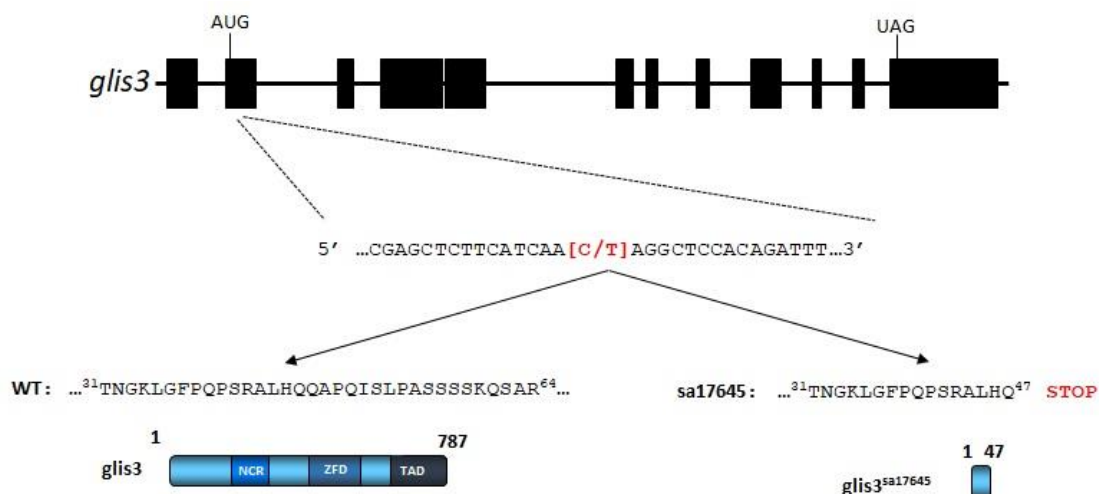
Figure 6. Schematic of the glis3$^{+/sa17645}$ mutant. Shaded rectangles indicate exons of the glis3 gene. Relative positions of the start and stop codons are indicated. The mutated region in exon 2 found in glis3^{sa17645} zebrafish is shown in detail. The wild type glis3 product is comprised of 787 amino acids while the glis3^{sa17645} nonsense mutation prematurely truncates the protein at Gln47. NCR = N-terminal conserved region; ZFD = zinc-finger domain; TAD = transactivation domain.

Zebrafish Breeding

In order to obtain a complete glis3 knockout model, the heterozygous glis3$^{+/sa17645}$

mutants were intercrossed. Following the development of glis3$^{sa17645/\ sa17645}$ males, these

where then crossed with heterozygous glis3$^{+/sa17645}$ females to increase the yield of

glis3$^{sa17645/\ sa17645}$ mutants. Zebrafish breeding protocol has been previously described

(Naiadka and Clark 2012). Briefly, 1 female and 2-3 males are placed in a 1.0 L

AQUANEERING crossing tank with a divider overnight. At the onset of the light cycle

the divider is removed and zebrafish are allowed to spawn and fertilize the eggs, which

fall through the slotted bottom of the inner tank. After spawning, the eggs are removed

and placed in E2 media until hatched (approximately 5 dpf).

After hatching, larval fish are placed in a 1.8 L still water nursery tank at no more than 50 larval fish per tank (Vargesson 2007). Larval fish are fed concentrated ground paramecia until 9 dpf. Following 9 dpf, larval fish are transferred to the continuous flow system, and fed ZIRC Nursery Mix twice daily until 21 dpf. At 21 dpf the larval diet is switched to the standard GEMMA Micro food supplemented with ZIRC Nursery Mix once daily until 45 dpf, at which point the larval fish begin to follow the adult dietary protocol outlined above.

TaqMan SNP Genotyping Assays

TaqMan SNP genotyping assays were used to verify the genotype of offspring generated by glis3$^{+/sa17645}$ x glis3$^{+/sa17645}$ crosses. 90-day old fish where anesthetized using tricaine-S and tail clippings where taken. Anesthetization by tricaine has been previously described (Matthews and Varga 2012). Before tail clipping, zebrafish were weighed and measured to determine if a reduction or loss of glis3 during development effected phenotypic body size. After tail clipping, zebrafish where kept in isolation for ten days to allow their tail to regrow, and then where sorted into tanks with siblings that shared genotype. DNA from tail clippings was extracted using HotSHOT DNA extraction (Meeker et al. 2007).

Site directed mutagenesis was used to create the hypothesized C/T mutation in wildtype zebrafish DNA in order to use as a positive control for the TaqMan SNP genotyping assays. Wildtype glis3 was generated by PCR amplification using the drglis3 EcoRI IN and drglis3 BamHI OUT primers and inserted into the pCRII-TOPO plasmid. The glis3-pCRII-TOPO plasmid was inserted into DH5α cells grown on Amp$^+$ LB

culture plates. Colonies were selected and cleaned using a plasmid miniprep kit (ThermoFisher) using the manufacturer's protocol.

Wildtype glis3 DNA was then mutated using the glis3 sa17645 C>T F and glis3 sa17645 C>T R primers and PFU Turbo DNA polymerase. glis3-pCRII-TOPO plasmid DNA was incubated in the restriction enzyme Dpn I to remove unmutated DNA. Mutated DNA was then transfected into XL10-Gold competent cells and grown on AMP$^+$ LB culture plates. Colonies were selected and cleaned using a plasmid miniprep kit (ThermoFisher) using the manufacturer's protocol. Mutated DNA was removed from the glis3-pCRII-TOPO plasmid using the restriction enzyme EcoRI. Mutation was verified by sequencing.

Primer Name	Primer Sequence (5' to 3')
drglis3 EcoRI IN	ATGCGAATTCAGCTCAGATATCTCCA
drglis3 BamHI OUT	GTCAGGATCCTCAGCCTTCAGTGAA
glis3 sa17645 C>T F	CCGAGCTCTTCATCAATAGGCTCCACAGATTTC
glis3 sa17645 C>T R	GAAATCTGTGGAGCCTATTGATGAAGAGCTCGG

Table 1. List of primers used for site directed mutagenesis of glis3.

Wildtype zebrafish DNA, heterozygous glis3$^{+/sa17645}$ DNA, and the mutated glis3$^{sa17645/sa17645}$ DNA were used as positive controls for genotyping the glis3$^{+/sa17645}$ x glis3$^{+/sa17645}$ cross offspring. TaqMan SNP genotyping assays use two probes that differ in sequence only at the SNP site. Each probe contains a covalent linked 5' reported dye and 3' quencher dye (Fig. 7). While the probe is intact, the quencher dye suppresses the signal of the reporter dye. Cleaving of the reporter and quencher dyes is accomplished by Taq polymerase if the probe and DNA are exactly complimentary. If the pairing is off by one nucleotide because of the SNP, then the probe is dislodged and the reported dye signal is

not received. By comparing the ratio of the signal received from the two reporter dyes, it

is possible to determine the ratio of the genes expressed.
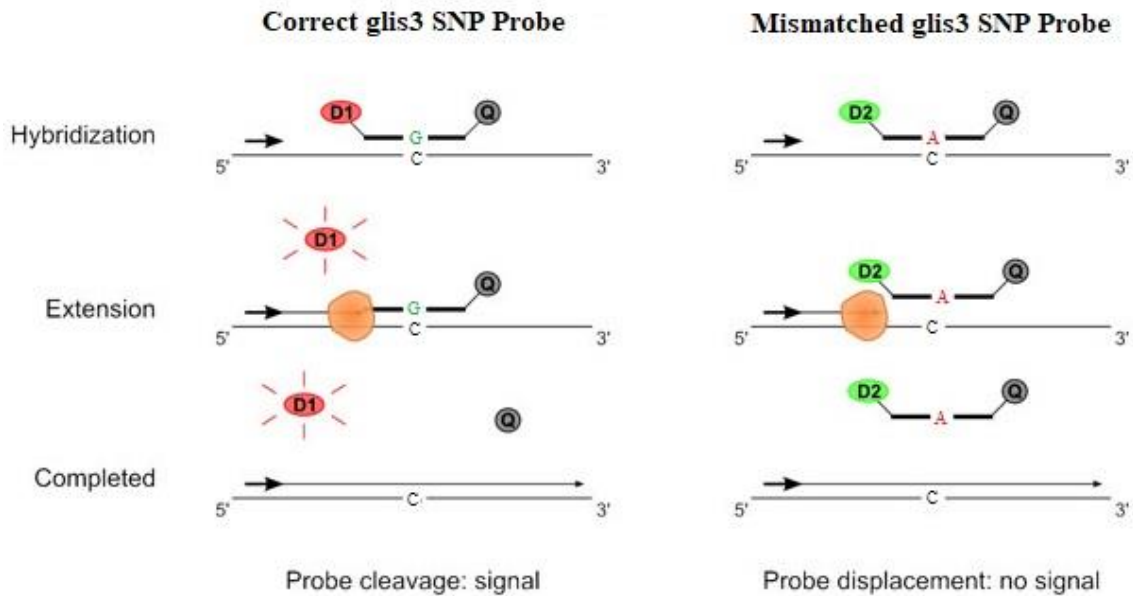
Figure 7. Schematic of the mechanism of TaqMan SNP genotyping assays. D1 and D2
are the reporter dyes for the separate probes. Q is the quencher dye, the orange circle is
Taq polymerase, and the dark arrow are the forward primers. (Adapted from
http://www.applied-maths.com/applications/taqman-based-snp-genotyping).

Blood Glucose Determination

The method for measuring blood glucose levels in zebrafish have been previously

described (Eames et al. 2010). Briefly, fish are anesthetized in water at 0 °C, as tricaine-S

anesthetization interferes with glucose levels (Eames et al. 2010, Matthews and Varga

2012). Fish are then decapitated, and blood glucose is measured using the FreeStyle Lite

Blood Glucose and Monitoring System. Blood glucose measurements were taken for

wildtype and glis3$^{+/sa17645}$ heterozygotes while fasting, post prandially, and following

application of a high fat, high glucose diet.

To simulate a high fat diet (HFD) that leads to the onset of diabetes, 3 wildtype and 3 glis3$^{+/sa17645}$ fish where submerged in 10.0 g of 99% D-glucose (Sigma-Aldrich) dissolved in 500 ml of system water. They were then fed 0.1 grams of powdered chicken egg yolk (Sigma-Aldrich) in supplement to their normal diet. This regiment was repeated 3 times a week for 4 months.

After the measurement of blood glucose levels, fasting and postprandial fish where dissected to determine the concentration of glis3, insa, gcga, and gcgb in the pancreas, kidney, brain, and gonads. Fish exposed to the HFD where fixed in 4% paraformaldehyde (PFA) and mounted in Paraplast X-TRA for sectioning to determine if reduction in glis3 effected β cell mass expansion in response to nutrient excess.

Quantitative Reverse Transcriptase Real-Time PCR Analysis

RNA was isolated from wildtype eggs or wildtype and glis3$^{+/sa17645}$ heterozygote organs using TRIzol RNA Extraction (Simms et al. 1993). Equal amounts of RNA were used to generate cDNA using a high capacity cDNA kit (Applied Biosystems). cDNA was then analyzed by quantitative real time PCR using the PowerUP SYBR green master mix (ThermoFisher Scientific). All qRT-PCR was performed using the Applied Biosystems 7500 real time PCR system. Primers used during RT-PCR are listed below (Table 2). GapDH and eIF1A were used to normalize RNA levels across different cell types and ages.

Immunohistochemistry and Microscopy

Zebrafish gut sections where fixed in 4% paraformaldehyde for 3 hours and washed in PBS. Tissue samples where then dehydrated with serial dilutions of ethanol in DEPC water with increasing amounts of ethanol. Tissue samples were infiltrated with

Gene Target	Primer Sequence (5' to 3')
glis3	F- ATGCGAATTCAGCTCAGATATCTCCA
	R- GTCAGGATCCTCAGCCTTCAGTGAA
insa	F- CTGTGTGGATCTCATCTGGT
	R- CTCTCTTCCTTATCAGCTCG
gcga	F- CGACAGCACAAGCACAGAGACAG
	R- GACGTTTGACAGAACCACCATTTC
gcgb	F- GGAAAACGGCAGCCTTATGTCTG
	R- CGTGTCGGGACTCCACTCCTCT
gapdh	F- CGTCTGGTGACCCGTGCTGCTTT
	R – AGTGGAGGCTGGGATGATGTTCT

Table 2. List of primers used for RT-PCR.

Hemo-De and decreasing concentrations of ethanol. After infiltration, gut tissues where incubated at 65º C in 50% Hemo-De/50% Paraplast X-TRA (Sigma-Aldrich) for one hour, and then 100% Paraplast X-TRA at 65º C overnight. Tissue samples where then embedded in Paraplast X-TRA and allowed to cool overnight.

Paraplast blocks were sectioned into 20 um samples using the Spencer 820 Rotary Microtome and mounted on Superfrost Plus microscope slides (Fisherbrand). Mounted paraplast sections were allowed to dry at RT overnight. Sections were rehydrated in serial dilutions of ethanol with decreasing concentrations of alcohol. After rehydration of tissue sections, antigen retrieval was performed on slides preceding immune histochemical staining began. Both enzymatic (Shi et al. 1997) and heat-mediated antigen retrieval (Norton et al. 1994, von Wasielewski et al. 1994) were attempted.

For enzymatic antigen retrieval, slides were blotted dry and individual samples were enclosed with a hydrophobic barrier pap pen (Aqua Hold II). 100 ul of prewarmed 0.05% trypsin was applied to each sample, and then incubated at 37º C for 20 minutes. Samples where then rinsed with running water for three minutes. For heat-mediated antigen retrieval, slides were immersed in Sodium Citrate Buffer (10mM Sodium Citrate,

0.05% Tween 20, pH 6.0) heated to 100º C for 20 minutes. Samples were then rinsed with cold running tap water for 10 minutes.

Slides were rinsed in TBS plus 0.025% Triton X-100 with gentle agitation and blocked with 10% normal sheep serum with 1% bovine serum albumin (BSA) in TBS for 2 hours at RT. Slides where then drained and again enclosed with the hydrophobic barrier pap pen and incubated over night at 4º C in 100 ul of 7 ug/ml Monoclonal Anti-Glucagon antibodies grown in mouse (Sigma) and 5 ug/ml Rb pAb to insulin (Abcam) primary antibody diluted in TBS with 1% BSA. Slides where then rinsed in TBS 0.025% Triton with gentle agitation. Tissues were then stained with 100 ul of 4 ug/ml anti-rabbit AlexaFluor 594 secondary antibody (ThermoFisher Scientific) and 4 ug/ml anti-mouse AlexaFluor 488 secondary antibody (ThermoFisher Scientific) for 1 hour at RT in the dark. Slides where then rinsed in TBS and mounted using Prolong Diamond anti-fade with DAPI (Life Technologies) and sealed with clear nail polish. Slides where observed using a Leica DMi8 fluorescence inverted microscope (Leica Microsystems) and images where captured using a DFC7000T cooled fluorescence camera and LAS X Expert software (Leica Microsystems).

Results

glis3 Expression Begins After 14.5 hpf in Wildtype Zebrafish

In order to determine when glis3 RNA transcription begins in wildtype zebrafish, total RNA was harvested from zebrafish eggs every two hours during development, starting at 5 hpf when maternal RNA is degraded (Abrams and Mullins 2009). The total RNA was converted into cDNA and used in quantitative reverse transcriptase real-time PCR analysis (qRT-PCR) to determine glis3 RNA expression levels. In addition, the expression of insa and pdx 1 RNA levels were measured as positive controls, as it is known that Pdx 1 expression begins at 13 hpf (Kimmel et al. 2011) and insa expression begins approximately 17 hpf (Papasani et al. 2006). Expression of glis3 was shown to begin after 14.5 hpf (Fig. 8), as measured by a significant change ($p < 0.05$) in expression levels from 5 hpf, where the transition from maternal to zygotic RNA expression begins (Abrams and Mullins 2009). Glis3 expression increased significantly again at E18.5 exhibiting a 3.5-fold increase in expression. During this experiment, the positive controls of pdx 1 and insa both show transcription start times where they have been previously recorded, from 11-14.5 hpf and 16.5-18.5 hpf, respectively.

glis3[sa17645] Zebrafish are Viable but Sex Determination May be Affected

The glis3[+/sa17645] mutants described above were intercrossed in an attempt to generate a line of zebrafish with a ubiquitous knockout of glis3. The genotype of offspring generated by this glis3[+/sa17645] x glis3[+/sa17645] cross was determined using TaqMan SNP Genotyping assays. Comparison of the ratio of magnitude of two separate reporter dyes was used to determine the ratio of genes expressed in the offspring genome

(Fig. 9). Each reporter dye was specific to a certain SNP in the region being examined, so homozygotes for either allele would show high expression of one probe and no expression of the other. Heterozygous glis$^{3+/sa17645}$ fish showed near
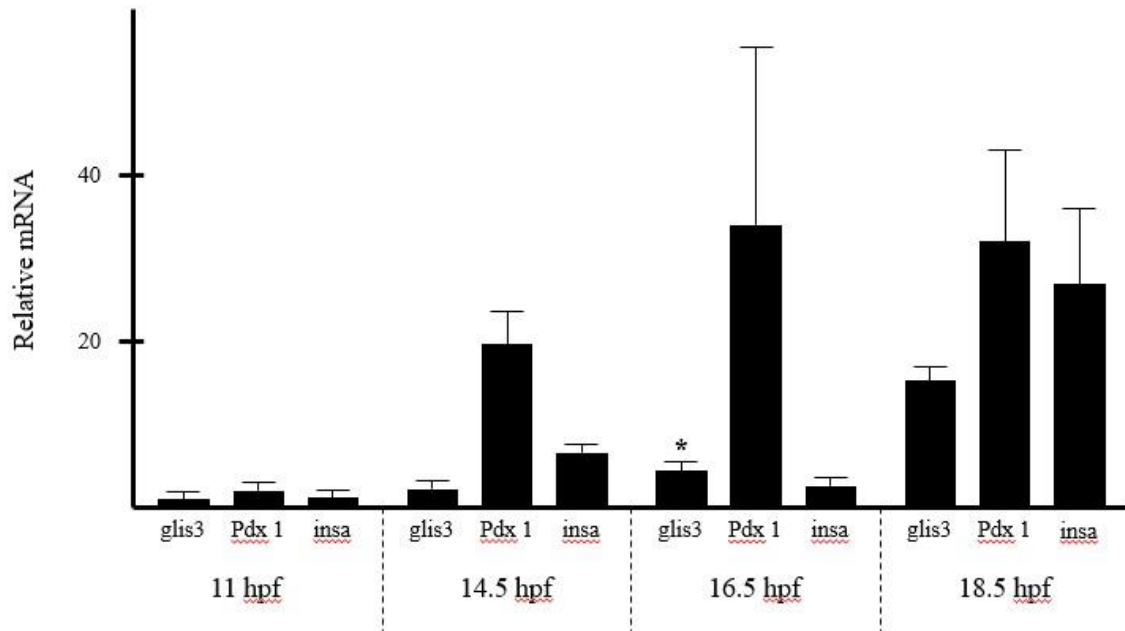
Figure 8. Expression of mRNA levels during development of zebrafish embryos. qRT-PCR was used along with PowerUP SYBR green to determine the beginning of RNA expression of multiple transcription factors. Pdx1 and insa are used as positives controls with expression beginning at 13 hpf and 17 hpf, respectively. glis3 expression was shown to differ from time points without expression (represented by *) at 16.5 hpf (p=0.017), indicating that glis3 RNA expression begins sometime after 14.5 hpf. All RNA levels where normalized against eIF1A expression levels.

equivalent expression of both probes. The genotypic and gender ratio of the performed crosses were examined for any abnormalities that may be caused by the lack of glis3 expression during development (Table 3). The observed genotypic ratio was compared to the expected 1:2:1 ratio using the Chi Squared test (χ^2) and a χ^2 value of 1.628 was determined for the offspring genotypes. With two degrees of freedom, this means that the observed genotypic ratio is not statistically different from the hypothetical ratio (p=0.443). When comparing the gender ratio, a χ^2 value of 4.829 was obtained, which

indicates a significant difference in the expected gender ratio (p=0.028). However, until

the line is further developed it is difficult to determine if this is a biologically significant

difference or if difficulty in determining the sex of young adult zebrafish has skewed this

data. Interestingly, the gender ratio is skewed more highly with reduction of glis3, while

wildtype exhibit the expected 1:1 ratio. Unfortunately, the cause behind gender

specification in zebrafish is complex (von Hofsten and Olsson 2005), so further research

is needed in order to determine if the deletion of glis3 may have an effect on the gender

ratio of zebrafish.

Figure 9. Determination of offspring genotype. A glis3$^{+/sa17645}$ x glis3$^{+/sa17645}$ cross was performed and DNA samples were taken using the HotSHOT DNA isolation method. Samples were run in duplicate using TaqMan SNP Genotyping assays to determine offspring genotype. Analysis of signaling dye ratio was done automatically using built in TaqMan Genotyper Software.
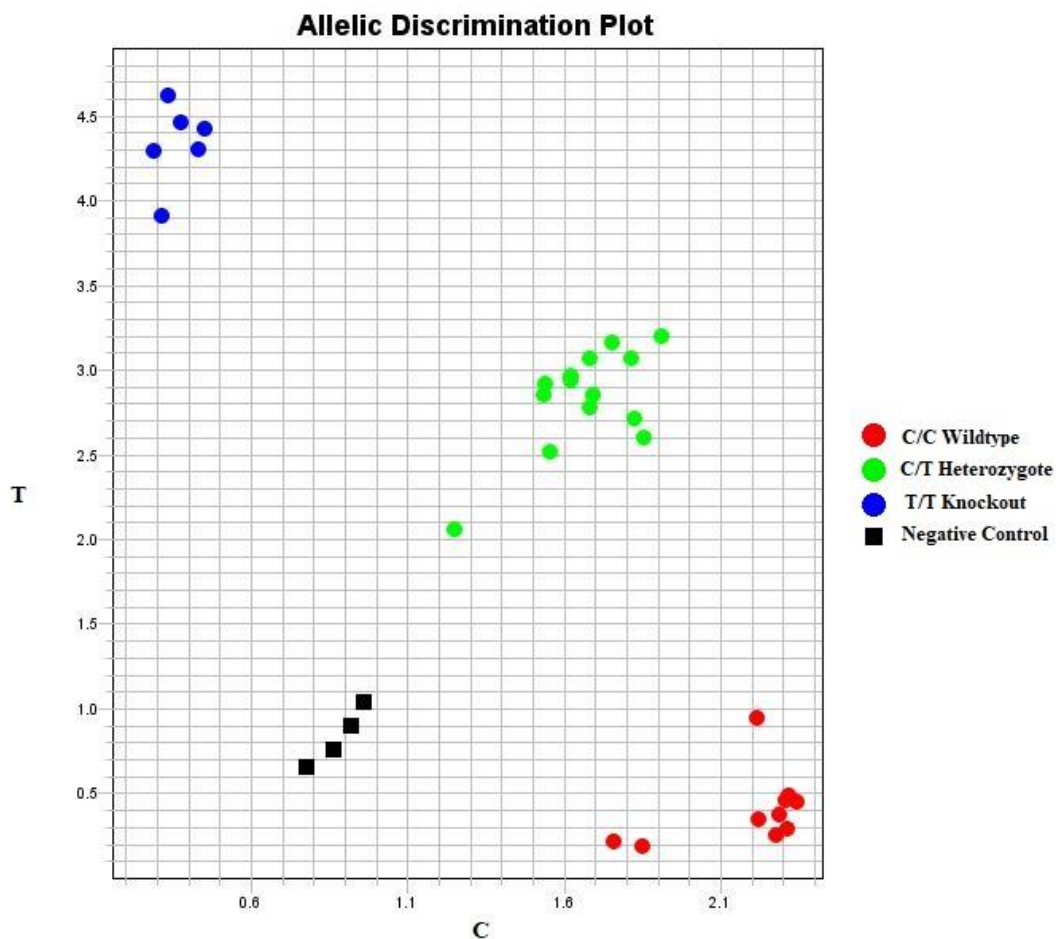
Gender	glis3$^{+/+}$	glis3$^{+/sa17645}$	glis3$^{sa17645/sa17645}$
Male	4	14	6
Female	4	7	0

Table 3. Examination of genotypic and gender ratios of offspring. A glis3$^{+/sa17645}$ x glis3$^{+/sa17645}$ cross was performed, resulting in 8 glis3$^{+/+}$ offspring, 21 glis3$^{+/sa17645}$ offspring, and 6 glis3$^{sa17645/sa17645}$ offspring. This genotypic ratio is not significantly different from the expected model for heritable genes (p=0.443). The gender ratio is skewed toward males in the mutant models, with not knockout females, but with n=6 it is impossible to determine if this is significant until the line is further developed.

While zebrafish were anesthetized for genotyping, and before sacrificing fish to determine blood glucose levels, mass and body length where measured to determine if glis3 mutation had any effect of the development of zebrafish growth. In order to account for differences in the size of male and female zebrafish and differences in size due to age, overall growth is measured as body mass index (BMI), or mass/length in g/mm. Using the body size measurements of 63 fish with a mix of all three genotypes, it was found that the reduction or deletion of glis3 does not have any significant effect on the development of zebrafish in regard to overall BMI (Fig. 10). Both heterozygous (p=0.228) and glis3$^{sa17645/sa17645}$ knockouts (p=0.068) show no significant deviation from average size of wildtype zebrafish. The borderline p-value of glis3$^{sa17645/sa17645}$ knockouts when compared to wildtype zebrafish is likely due to the low sample size (n=6) of glis3 knockout BMI and will be further scrutinized once the line is further developed.

Reduction of glis3 May Increase Blood Glucose Regulation Efficiency

Wildtype and glis3$^{+/sa17645}$ zebrafish had their blood glucose monitored under different dietary conditions in order to determine if a reduction in glis3 expression had any effect on blood glucose homeostasis (Fig. 11). Zebrafish were anesthetized in ice water as tricaine-S anesthetization interferes with glucose levels (Eames et al. 2010, Matthews and Varga 2012). Fish where then sacrificed, and blood glucose was measured
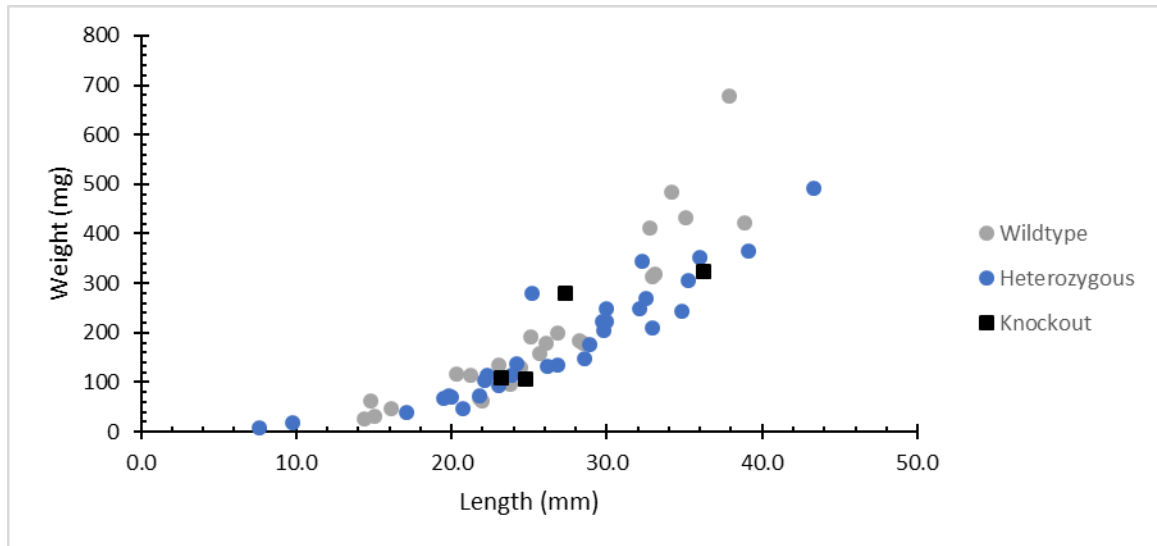
Figure 10. glis3 reduction does not affect zebrafish body mass index. Wildtype zebrafish have an average BMI of 6.80 x 10^{-3} ± 3.95 x10^{-3} g/mm (n=24). Using a two-sided t-test, the average BMI of the glis3$^{+/sa17645}$ and glis3$^{sa17645/sa17645}$ were shown to not be significantly different (p=0.228 and 0.068, respectively).

using the FreeStyle Lite Blood Glucose and Monitoring System. Baseline glucose levels where taken in fasting zebrafish, and immediate glucose response was measured in postprandial zebrafish. After four months of exposure to the high fat/high glucose diet described previously, resting blood glucose was then measured in wildtype and heterozygous fish in order to measure their ability to regulate blood glucose in response to nutrient excess.

The control diet wildtype and glis3$^{+/sa17645}$ showed a statistically significant difference in resting blood glucose levels (p=0.033). Neither the postprandial or HFD dietary groups show any significant different between blood glucose levels of the wildtype and heterozygous fish, though in the case of the HFD fish, this is likely due to the high fluctuations in blood glucose levels in the WT fish (p=0.142) In the HFD case the heterozygous fish expressed less variability in blood glucose (relative standard
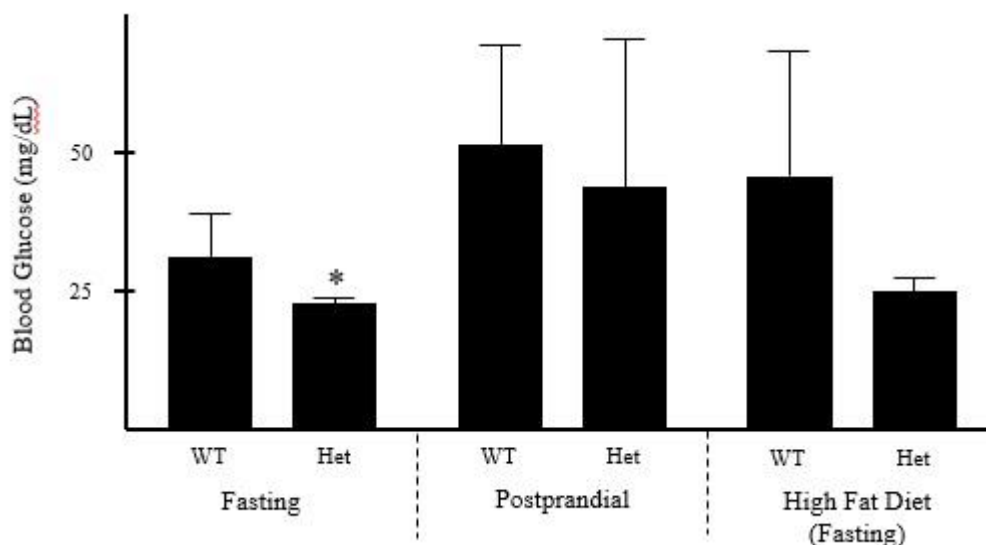
Figure 11. Blood glucose levels of fish with different dietary constraints. Blood glucose measurements were taken from fasting and postprandial control fish. Fasting heterozygotes exhibit lower resting blood glucose than wildtype counterparts (p=0.033). Fish exposed to a high fat diet (HFD) where then fasted and had resting blood glucose measurements take to determine if long term exposure to nutrient excess affected blood glucose homeostasis. There was no statistical significance in the difference in blood glucose levels between WT and heterozygous fish (p=0.142), though this is believed to be due to the high variability in in the WT fish, which were beginning to exhibit signs of T2DM. There was also no significant difference in the resting blood glucose levels of the control and HFD heterozygous fish (p=0.354). All blood glucose was measured using the FreeStyle Lite Blood Glucose and Monitoring System.

deviation = 0.10). Wildtype fish exposed to the HFD exhibit less efficient blood glucose

regulation in comparison to wildtype controls, which may be an indicator for the onset of

T2DM, while glis3$^{+/sa1645}$ fish showed no change in resting blood glucose levels

(p=0.354).

glis3 Heterozygotes Express Increased Levels of Islet Hormones

RNA expression levels where measured in the pancreas and brain of wildtype and

glis3$^{+/sa17645}$ heterozygotes under differing dietary constraints (Fig. 12). Total RNA was

collected using TRIzol RNA extraction. Equal amounts of RNA were used to generate

cDNA using a high capacity cDNA kit (Applied Biosystems). cDNA was then analyzed

by quantitative real time PCR. In both fasting and postprandial conditions, heterozygotes expressed increased levels of the primary islet hormone insulin (p<0.005 and p=0.033, respectively). Under postprandial condition, heterozygotes also displayed increased expression of glucagon (p=0.024).
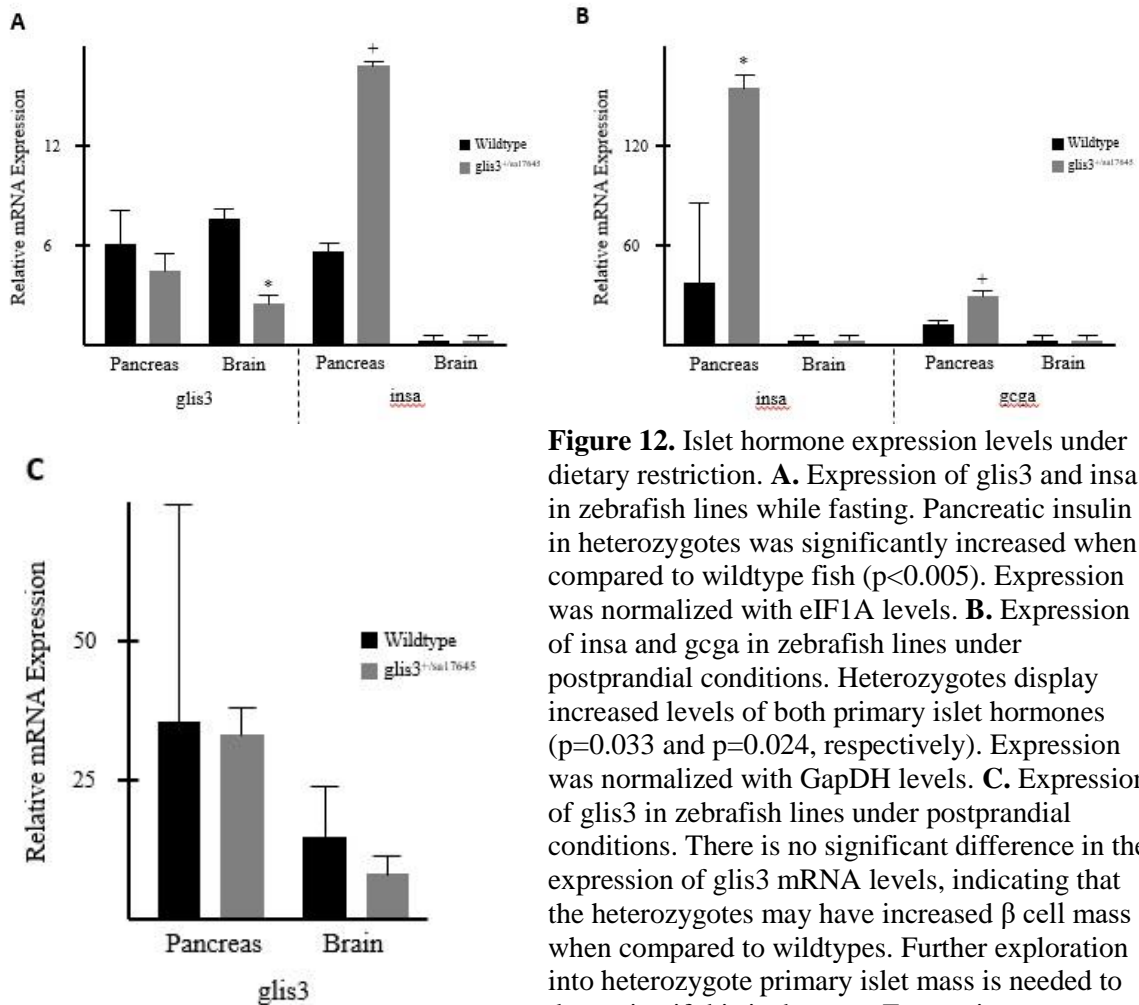
Figure 12. Islet hormone expression levels under dietary restriction. **A.** Expression of glis3 and insa in zebrafish lines while fasting. Pancreatic insulin in heterozygotes was significantly increased when compared to wildtype fish (p<0.005). Expression was normalized with eIF1A levels. **B.** Expression of insa and gcga in zebrafish lines under postprandial conditions. Heterozygotes display increased levels of both primary islet hormones (p=0.033 and p=0.024, respectively). Expression was normalized with GapDH levels. **C.** Expression of glis3 in zebrafish lines under postprandial conditions. There is no significant difference in the expression of glis3 mRNA levels, indicating that the heterozygotes may have increased β cell mass when compared to wildtypes. Further exploration into heterozygote primary islet mass is needed to determine if this is the case. Expression was normalized using GapDH expression levels.

Zebrafish Display Increased Islet Hormones in Response to HFD

Wildtype and glis3[+/sa17645] heterozygote fish were submerged in 0.1 M glucose and fed 0.1 g of powdered chicken egg yolk three times a week for four months in addition to their normal diet to simulate a high fat, high glucose diet. Blood glucose was

measured using the FreeStyle Lite Blood Glucose and Monitoring System (Fig. 11), and

TRIzol RNA extraction was used along side RT-PCR to determine RNA expression

levels in fish in response to the high fate diet (Fig. 13). Wildtype fish exposed to a high

fat diet showed no change in RNA expression of glis3 or gcga when compared to

wildtypes under normal dietary conditions. Heterozygotes exposed to high fat diet

displayed increased levels of insa (p=0.007) and gcga (p=0.019) when compared to

wildtype controls (Fig. 13). Heterozygotes show the expected reduced expression of glis3

in the brain (p=0.013), but do not express reduced glis3 levels in the pancreas. The

wildtype fish exposed to the high fat diet exhibit extremely reduced glis3 expression in

the brain, but this is likely due to the low sample size (n=1).
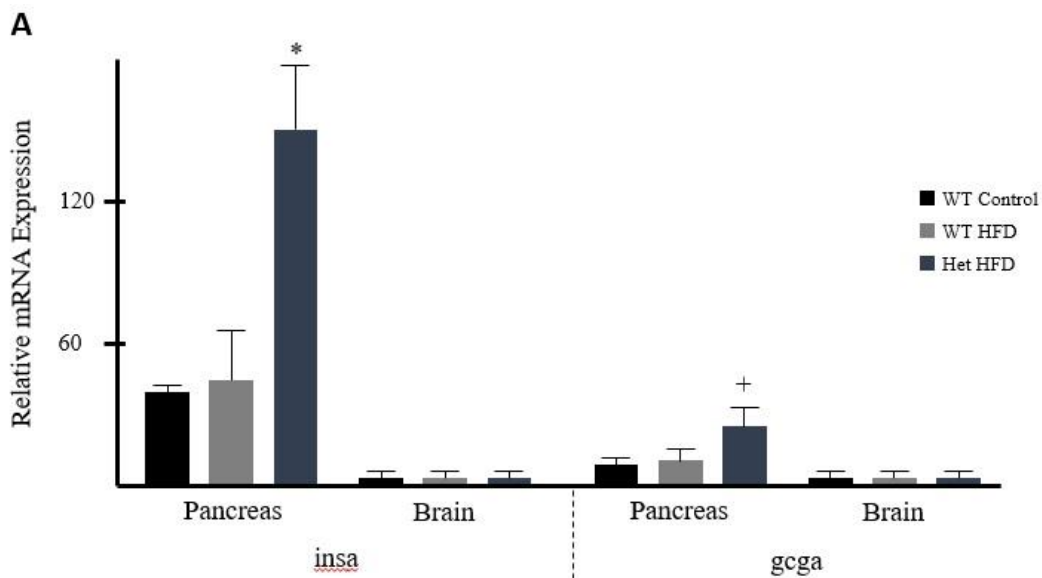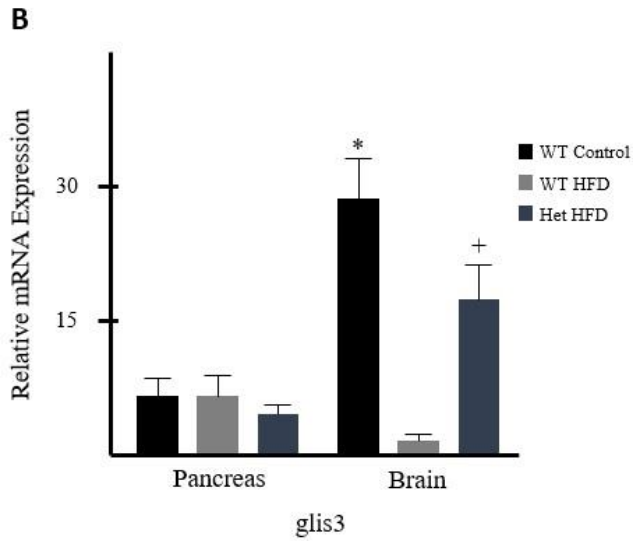
Figure 13. RNA expression levels in response to a high fat diet. **A.** Expression levels of insa and gcga in zebrafish. WT fish under normal dietary conditions where used as a control. glis3$^{+/sa17645}$ fish exhibit increased insa (p=0.007) and gcga (p=0.019) expression. All RNA expression was normalized using GapDH. **B.** Expression of glis3 was measured in fish in response to nutrient excess. Heterozygotes show the expected reduced glis3 levels in the pancreas (p=0.014), but not in the pancreas (p=0.064). All RNA levels were controlled for using GapDH.

Discussion and Future Direction

These studies have shown that glis3 expression levels in zebrafish have a significant impact on the expression levels of primary islet hormones. Zebrafish with decreased levels of glis3 exhibit increased production of insa and gcga mRNA, and glis3$^{+/sa17645}$ zebrafish exhibit an increased ability to regulate blood glucose. This is consistent with previous results that show that overexpression of glis3 in β cells causes a reduction in insulin levels, but directly in contrast to the idea that Glis3 is responsible for promoting insulin transcription in mice and humans (Kim et al. 2003, Senee et al. 2006, Kang et al. 2009, Yang et al. 2009, Yang et al. 2013b). These data indicate that glis3 might be acting as a repressor of insulin transcription in zebrafish, despite glis3 acting as a potent activator of insulin transcription *in vitro* (Kang et al. 2009, Watanabe et al. 2009, Yang et al. 2009, Yang et al. 2013b).

The increased expression of primary islet hormones in glis3 heterozygous zebrafish is indicative of glis3 repression of insa and gcga, which agrees with reporter studies indicating glis3 may act to inhibit insulin transcription. This may be due to glis3 playing a role in the prevention of differentiation into α and β cells, thus loss of glis3 might result in islet hyperplasia. This idea needs to be examined through immunohistochemical staining of islets in HFD challenged heterozygotes. Using whole mount *in situ* hybridization it can be shown that glis3 expression does not begin in the pancreatic region until approximately 48 hpf, which is 24 hours after pancreas development begins in zebrafish. Zebrafish glis3 expression begins after 14.5 hpf (Fig. 8), but early expression is restricted to the brain. The late expression of gli3 in the

pancreas, coupled with the changes in islet hormone levels in adulthood, may indicate that glis3 is required for stopping the signal that induces islet cell formation, or for controlling islet cell proliferation during β cell mass expansion.

Despite the fact that Glis3 has been identifies as a risk locus for the development of T1DM and T2DM in humans (Barrett et al. 2009, Boesgaard et al. 2010, Dupuis et al. 2010) Initial studies of the phenotype of glis3$^{+/sa17645}$ and glis3$^{sa17645/sa17645}$ fish indicate that loss of glis3 is having no negative impact on physiological health. This is similar to Medaka glis3 alternative splice isoform models, which displayed none of the symptoms of a pancreatic phenotype (Hashimoto et al. 2009). Glis3 heterozygous and knockout fish have exhibited normal feeding and breeding patterns, and no difference in BMI has been detected. The only appreciable difference in heterozygote and wildtype fish is the gender ratio of their offspring. In the initial steps of producing a complete glis3 knockout line, it has become apparent that reduction or loss of glis3 may increase the likelihood of male progeny. Further exploration of the gender of the glis3$^{+/sa17656}$ x glis3$^{+/sa17656}$ line is needed to determine if this biologically significant, or if this discrepancy is due to a low sample size. The mechanisms for zebrafish sex determination are currently unknown (von Hofsten and Olsson 2005), so an increased propensity towards male offspring in glis3 mutants would be a novel discovery toward understanding these mechanisms.

Furthermore, although the sample size is too small to be conclusive, glis3$^{+/sa1645}$ zebrafish seem to exhibit tighter regulation of blood glucose homeostasis than compared to wildtype fish (Fig. 11). In response to a high fat diet pancreatic glis3, insulin, and gcga expression levels in glis3$^{+/sa17645}$ zebrafish increase compared to wildtypes, while blood glucose levels remain normal. The resting blood glucose of wildtype zebrafish exposed to

a high fat diet increases, while insulin expression levels remain constant. Since the wildtype zebrafish are exhibiting the early symptoms of T2DM while the heterozygous remain healthy, we again posit that the reduction in glis3 may be aiding in the maintenance of healthy primary islets. Preliminary data indicates that glis3 heterozygotes may be more likely to begin the routine mechanism for compensatory β cell mass expansion or exhibit an increased production of insulin in existing cells. However, since glis3 is not expressed in the α cells of the pancreas, increased gcga production suggests an increase in islet mass. The lack of a significant change in glis3 expression levels in the pancreas of heterozygous and wildtype zebrafish lines may also be indicative of an increase in primary islet mass, as an increase in the number of β cells would lead to increased glis3 expression.

For a more in depth look at the role that glis3 plays in pancreatic function and maintenance, the generation of the complete glis3$^{sa17645/sa17645}$ knockout model will be continued. Analysis of glis3, insa, and gcga levels will be repeated for the glis3 knockout model under fasting and postprandial condition to determine if the loss of glis3 continues the trend of increased pancreatic hormone levels with decreased glis3 levels. Knockout glis3 mutants will be exposed to the high fat, high glucose diet and blood glucose and pancreatic hormone levels will be monitored to determine if loss of glis3 makes zebrafish more likely to develop T2DM.

Collectively, these studies have indicated that zebrafish glis3 may act as a repressor of insulin transcription. The increased likelihood of glis3$^{+/sa17645}$ to undergo a compensatory mechanism for β cell mass expansion in response to nutrient excess may lead to the development of models for the study of T2DM. Investigation of pancreas

morphology and hormone expression in response to loss of glis3 in environments of nutrient excess will be a continued focus of research in the future.

Literature Cited

1. Abrams EW, Mullins MC (2009) Early zebrafish development: it's in the maternal genes. Curr Opin Genet Dev 19(4): 396-403.
2. Agata Y, Matsuda E, Shimizu A (1999) Two novel Kruppel associated box-containing zinc-finger proteins, KRAZ1 and KRAZ2, repress transcription through functional interaction with the corepressor KAP-1 (TIF1beta/KRIP-1). J Biol Chem 274: 16412-16422.
3. Alpert S, Hanahan D, Teitelman G (1988) Hybrid insulin genes reveal a developmental lineage for pancreatic endocrine cells and imply a relationship with neurons. Cell 53: 295-308.
4. Andralojc KM, Mercalli A, Nowak KW, Albarello L, Calcagno R, Luzi L, Bonifacio E, Doglioni C, Piemonti L (2009) Ghrelin-producing epsilon cells in the developing and adult human pancreas. Diaboltegia 52(3): 486-493.
5. Aramata S, Han SI, Kataoka K (2007) Roles and regulation of transcription factor MafA in islet β-cells. Endocr J 54: 659-666.
6. Argenton F, Arava Y, Aronheim A, Walker MD (1996) An activation domain of the helix-loop-helix transcritption factor E2A show cell type preference in vivo in microinjected zebra fish embryos. Mol Cell Biol 16: 1714-1721.
7. Argenton F, Walker MD, Colombi L, Borolussi M (1997) Functional characterization of the trout insulin promoter: implications for fish as a favorable model of pancreas development. FEBS Lett 407: 191-196.
8. Argenton F, Zecchun E, Bortolussi M (1999) Early appearance of pancreatic hormone-expressing cells in zebrafish embryos. Mech Dev 87: 217-221.
9. Arystarkhova E, Liu YB, Salazar C, Stanojevic V, Clifford RJ, Kaplan JH, Kidder GM, Sweadner KJ (2013) Hyperplasia of pancreatic beta cells and improved glucose tolerance in mice deficient in the FXYD2 subunit of Na,K-ATPase. J Biol Chem 288(10): 7077-7098.
10. Attanasio M, Uhlenhaut NH, Sousa VH, O'Toole JF, Otto E, Anlag K, Klugmann C, Treier AC, Helou J, Sayer JA, Seelow D, Nürnberg G, Becker C, Chudley AE, Nürnberg P, Hildebrandt F, Treier M (2007) Loss of GLIS2 causes nephronophthisis in humans and mice by increased apoptosis and fibrosis. Nat Genet 39: 1018-1024.
11. Barrett JC, Clayton DG, Concannon P, Akolkar B, Cooper JD, Erlich HA, Julier C, Morahan G, Nerup J, Nierras C, Plagnol V, Pociot F, Schuilenburg H, Smyth DJ, Stevens H, Todd JA, Walker NM, Rich SS, The Type 1 Diabetes Genetics Consortium (2009) Genome-wide association study and metaanalysis find that over 40 loci affect risk of type 1 diabetes. Nat Genet 41: 703-707.
12. Bayha E, Jorgensen MC, Serup P, Grapin-Botton A (2009) Retinoic acid signaling organizes endodermal organ specification along the entire antero-posterior axis. PLoS ONE 4(6): e5845.

13. Beak JY, Kang HS, Kim YS, Jetten AM (2008) Functional analysis of the zinc finger and activation domains of Glis3 and mutant Glis3(NDH1). Nucleic Acids Res 36: 1690-1702.

14. Berbari NF, O'Connor AK, Haycraft CJ, Yoder BK (2009) The primary cilium as a complex signaling center. Curr Biol 19: R526535.

15. Biemar F, Argenton F, Schmidtke R, Epperlein S, Peers B, Driever W (2001) Pancreas development in zebrafish: early dispersed appearance of endocrine hormone expressing cells and their convergence to form the definitive islet. Dev Biol 230: 189-203.

16. Bisgrove BW, Yost HJ (2006). The roles of cilia in developmental disorders and disease. Development 133: 4131-4143.

17. Blader P, Lam CS, Rastegar S, Scardigli R, Nicod JC, Simplicio N, Plessy C, Fischer N, Schuurmans C, Guillemot F, Strahle U (2004) Conserved and acquired features of neurogenin1 regulation. Development 131: 5627-5637.

18. Boesgaard TW, Grarup N, Jorgensen T, Borch-Johnsen K, Hansen T, Pedersen O (2010) Variants at DGKB/TMEM195, ADRA2A, GLIS3 and C2CD4B loci are associated with reduced glucosestimulated beta cell function in middle-aged Danish people. Diabetologia 53: 1647-1655.

19. Bouwens L, Wang RN, De Blay E, Pipeleers DG, Kloppel G (1994) Cytokeratins as markers of ductal cell differentiation and islet neogenesis in the neonatal rat pancreas. Diabetes 43: 1279-1283.

20. Braun M, Ramracheya R, Bengtsson M, Zhang Q, Karanauskaite J, Partridge C, Johnson PR, Rorsman P (2008) Coltage-gated ino channels in human pancreatic beta-cells: electrophysiological characterization and role in insulin secretion. Diabetes 57(6): 1618-1628.

21. Corbit KC, Shyer AE, Dowdle WE, Gaulden J, Singla V, Chen MH, Chuang PT, Reiter JF (2008) Kif3a constrains betacatenin-dependent Wnt signalling through dual ciliary and non-ciliary mechanisms. Nat Cell Biol 10: 70-76.

22. Deutsch G, Jung J, Zheng M, Lora J, Zaret KS (2001) A bipotential precursor population for pancreas and liver within the embryonic endoderm. Development 128: 871-881.

23. Devos N, Deflorian G, Biemar F, Bortolussi M, Martial JA, Peers B, Argenton F (2002) Differential expression of two somatostatin genes during zebrafish embryonic development. Mech Dev 115: 133-137.

24. Dor Y, Brown J, Martinez OI, Melton DA (2004) Adult pancreatic beta-cells are formed by self-duplication rather than stem-cell differentiation. Nature 429:41-46.

25. Duan H, Skeath JB, Nguyen HT (2001) Drosophila Lame duck, a novel member of the Gli superfamily, acts as a key regulator of myogenesis by controlling fusion-competent myoblast development. Development 128: 4489-4500.

26. Dupuis J et al. (2010) New genetic loci implicated in fasting glucose homeostasis and their impact on type 2 diabetes risk. Nat Genet 42: 405416.

27. Eames SC, Philipson LH, Prince VE, Kinket MD (2010) Blood sugar measurement in zebrafish reveals dynamics of glucose homeostasis. Zebrafish 7(2): 205-213.

28. Elghazi L, Cras-Meneur C, Czernichow P, Scharfmann R (2002) Role for FGFR02IIIb-mediated signals in controlling pancreatic endocrine progenitor cell proliferation. Proc Natl Acad Sci USA 99: 3884-3889.

29. Enrico M, Gnugge L, Braghetta P, Bortolussi M, Argenton F (2009) Analysis of beta cell proliferation dynamics in zebrafish. Dev Biol 332(2): 299-308.

30. Fliegauf M, Benzing T, Omran H (2007) When cilia go bad: cilia defects and ciliopathies. Nat Rev Mol Cell Biol 8: 880-893.

31. Force A, Lynch M, Pickett FB, Amores A, Yan YL, Postlethwait J (1999) Preservation of duplicate genes by complementary, degenerative mutations. Genetics 151:1531-1545.

32. Furlong EE, Andersen EC, Null B, White KP, Scott MP (2001) Patterns of gene expression during Drosophila mesoderm development. Science 293: 1629-1633.

33. Garofano A, Czernichow P, Breant B (1998) Beta-cell mass and proliferation following late fetal and early postnatal malnutrition in the rat. Diabetologia 41: 1114-1120.

34. Gerdes JM, Davis EE, Katsanis N (2009) The vertebrate primary cilium in development, homeostasis, and disease. Cell 137: 32-45.

35. Goessling W, North TE, Lord AM, Ceol C, Lee S, Weidinger G, Bourque C, Strijbosch R, Haramis AP, Puder M, Clevers H, Moon RT, Zon LI (2008) APC mutant zebrafish uncover a changing temporal requirement for wnt signaling in liver development. Dev Biol 320: 161-174.

36. Golosow N, Grobstein C (1962) Epitheliomesenchymal interactions in pancreatic morphogenesis. Dev Biol 4: 242-255.

37. Goodison S, Kenna S, Ashcroft SJ (1992) Control of insulin gene expression by glucose. Biochem J 285(2): 563-568.

38. Gu G, Dubauskaite J, Melton DA (2002) Direct evidence for the pancreatic lineage: NGN3+ cells are islet progenitors and are distinct from duct progenitors. Development 129(10): 247-2457.

39. Hashimoto H, Miyamoto R, Watanabe N, Shiba D, Ozato K, Inoue C, Kubo Y, Koga A, Jindo T, Narita T, Naruse K, Ohishi K, Nogata K, Shin-I T, Asakawa S, Shimizu N, Miyamoto T, Mochizuki T, Yokoyama T, Hori H, Takeda H, Kohara Y, Wakamatsu Y (2009) Polycystic kidney disease in the medaka (Oryzias latipes) pc mutant caused by a mutation in the Gli-Similar3 (Glis3) gene. PLoS One 4: e6299.

40. Hattersley A, Bruining J, Shield J, Njolstrad P, Donaghue KC (2009) The diagnosis and management of mongenic diabetes in children and adolescents. Pediatr Diabetes 12: 33-42.

41. Haycraft CJ, Banizs B, Aydin-Son Y, Zhang Q, Michaud EJ, Yoder BK (2005) Gli2 and Gli3 localize to cilia and require the intraflagellar transport protein polaris for processing and function. PLoS Genet 1: e53.

42. Hebrok M, Kim SK, Melton DA (1998) Notochord repression on endodermal Sonic hedgehog permits pancreas development. Genes Dev 12: 1705-1713.

43. Hellerstrom C, Swenne I (1991) Functional maturation and proliferation of fetal pancreatic beta cells. Diabetes 40: 89-93.

44. Hong JH, Hwang ES, McManus MT, Ansterdam A, Tian Y, Kalmukova R, Mueller E, Benjamin T, Spiegelman BM, Sharp PA, Hopkins N, Yaffe MB (2005) TAZ, a transcriptional modulator of mesenchymal stem cell differentiation. Science 309(5737): 1074-1078.

45. Hong JH, Yaffe, MB (2006) Taz: a beta-catenin-like molecule that regulates mesenchymal stem cell differentiation. Cell Cycle 5(2): 176-179.

46. Hosking CR, Ulloa F, Hogan C, Ferber E, Figueroa A, Gevaert K, Birchmeier W, Briscoe J, Fujita Y (2007) The transcriptional repressor Glis2 is a novel binding partner for p120 catenin. Mol Biol Cell 18: 1918-1927.

47. Howe K, et al. (2013) The zebrafish reference genome sequence and its relationship to the human genome. Nature 496: 498-503.

48. Huang W, Beer RL, Delaspre F, Wang G, Edelman HE, Park H (2016) Sox9b is a mediator of retinoic acid signaling restricting endocrine progenitor differentiation. Dev Biol 418(1):28–39.

49. Kaneto H, Miyatsuka T, Fujitani Y, Noguchi H, Song KH, Yoon KH, Matsuoka TA (2007) Role of PDX-1 and MafA as a potential therapeutic target for diabetes. Diabetes Res Clin Pract 77: S127-S137.

50. Kang HS, Kim YS, ZeRuth G, Beak JY, Gerrish K, Kilic G, SosaPineda B, Jensen J, Foley J, Jetten AM (2009) Transcription factor Glis3, a novel critical player in the regulation of pancreatic beta-cell development and insulin gene expression. Mol Cell Biol 29: 6366-6379.

51. Kang HS, ZeRuth G, Lichti-Kaiser K, Vasanth S, Yin Z, Kim Y, Jetten AM (2010) Gli-similar (Glis) Krüppel-like zinc finger proteins: insights into their physiological functions and critical roles in neonatal diabete and cystic renal disease. Histol Histiopathol 25: 1481-1496.

52. Kataoka K (2007) Multiple mechanisms and functions of maf transcription factors in the regulation of tissue-specific genes. J Biochem 141: 775-781.

53. Kaung HL (1994) Growth dynamics of pancreatic islet cell populations during fetal and neonatal development of the rat. Dev Dyn 200: 163-175.

54. Kettleburough RNW, Busch-Nentwich EM, Harvey SA, Dooley CM, de Bruijn E, van Eeden F, Sealy I, White RJ, Herd C, Nijman IJ, Fényes F, Mehroke S, Scahill C, Gibbons R, Wali N, Carruthers S, Hall A, Yen J, Cuppen E, Stemple DL (2013) A systematic genome-wide analysis of zebrafish protein-coding gene function. Nature 496:494-499.

55. Kim YS, Lewandoski M, Perantoni AO, Kurebayashi S, Nakanishi G, Jetten AM (2002) Identification of Glis1, a novel Gli-related, Kruppel-like zinc finger protein containing transactivation and repressor functions. J Biol Chem 277: 30901-30913.

56. Kim YS, Nakanishi G, Lewandoski M, Jetten AM (2003) GLIS3, a novel member of the GLIS subfamily of Kruppel-like zinc finger proteins with repressor and activation functions. Nucleic Acids Res 3: 5513-5525.

57. Kim SC, Kim YS, Jetten AM (2005) Kruppel-like zinc finger protein Gli-similar 2 (Glis2) represses transcription through interaction with C-terminal binding protein 1 (CtBP1). Nucleic Acids Res 33: 6805-6815.

58. Kim J, Kato M, Beachy PA (2009) Gli2 trafficking links Hedgehog-dependent activation of Smoothened in the primary cilium to transcriptional activation in the nucleus. Proc Natl Acad Sci USA 106: 21666-21671.

59. Kimmel RA, Onder L, Wilfinger A, Ellertsdottir E, Meyer D (2011) Requirement for Pdx1 in specification of latent endocrine progenitors in zebrafish. BMC Biology 9:75.

60. Kinzler KW, Ruppert JM, Bigner SH, Vogelstein B (1988) The GLI gene is a member of the Kruppel family of zinc finger proteins. Nature 332: 371-374.

61. Lamar E, Kintner C, Goulding M (2001) Identification of NKL, a novel Gli-Kruppel zinc-finger protein that promotes neuronal differentiation. Development 128: 1335-1346.

62. Lammert E, Cleaver O, Melton D (2001) Induction of pancreatic differentiation by signals from blood vessels. Science 294: 564-567.

63. Lopez-Olmeda J, Madrid JA, Sanchez-Vasquez FJ (2006). Light and temperature cycle as zeitgerbers of zebrafish (*Danio rerio*) circadian activity rhythms. Chronobiol Int 23: 537-550.

64. Marcus EA, Kintner C, Harris W (1998) The role of GSK3β in regulating neuronal differentiation in Xenopus laevis. Mol Cell Neurosci 12: 269-280.

65. Matthews M, Varga ZM (2012) Anesthesia and euthanasia in zebrafish. ILAR Journal 53(2): 192-204.

66. McEvoy RC, Madson KL (1980) Pancreatic insulin-, glucagon-, and somatostatin-positive islet cell populations during the perinatal development of the rat. I Morphometric quantitation Biol Neonate 38: 248–254.

67. McLin VA, Rankin SA, Zorn AM (2007) Repression of Wnt/beta-catenin signaling in the anterior endoderm is essential for liver and pancreas development. Development 134(12): 2207-2217.

68. Meeker ND, Hutchinson SA, Ho L, Trede N (2007) Method for isolation of PCR-ready genomic DNA from zebrafish tissues. Bio Techniques 43: 610-614.

69. Melloul D, Marshak S, Cerasi E (2002) Regulation of insulin gene transcription. Diabetologia 45: 309-326.

70. Montanya E, Nacher V, Biarnes M, Soler J (2000) Linear correlation between beta-cell mass and body weight throughout the lifespan in Lewis rats: role of beta-cell hyperplasia and hypertrophy. Diabetes 49: 1341-1346.

71. Mosley AL, Ozcan S (2004) The pancreatic duodenal homeobox-1 protein (Pdx-1) interacts with histone deacetylases Hdac-1 and Hdac-2 on low levels of glucose. J Biol Chem 279: 54241-54247.

72. Moss JB, Koustunhan P, Greenman M, Parsons MJ, Walter I, Moss LG (2009) Regeneration of the pancreas in adult zebrafish. Diabetes 58: 1844-1851.

73. Nakashima M, Tanese N, Ito M, Auerbach W, Bai C, Furukawa T, Toyono T, Akamine A, Joyner AL (2002) A novel gene, GliH1, with homology to the Gli zinc finger domain not required for mouse development. Mech Dev 119: 21.

74. Nasiadka A, Clark MD (2012) Zebrafish breeding in the laboratory environment. ILAR J 53(2): 161-168.

75. Naya FJ, Huang H, Qiu Y, Mutoh H, DeMayo FJ, Leiter AB, Tsai M (1997) Diabetes, defective pancreatic morphogenesis, and abnormal enteroendocrine differentiation in BETA2/NeuroD-deficient mice. Genes Dev 11: 2323-2334.

76. Norton AJ, Jordan S, Yeomans P (1994) Brief, high-temperature denaturation (pressure cooking): a simple and effective method of antigen retrieval for routinely processed tissues. J Pathol 173(4): 371-379.

77. Ohneda K, Ee H, German M (2000) Regulation of insulin gene transcription. Semin Cell Dev Biol 11: 227-233.

78. O'Hare EA, Yerges-Armstrong LM, Perry JA, Shuldiner AR, Zaghloul NA (2016) Assignment of functional relevance to genes at type 2 diabetes-associated loci through investigation of beta-cell mass deficits. Mol Endocrinol 30: 429-445.

79. Oro AE (2007) The primary cilia, a 'Rab-id' transit system for hedgehog signaling. Curr Opin Cell Biol 19: 691-696.

80. Pack M, Solnica-Krezel L, Malicki J, Neuhauss SC, Schier AF, Stemple DL, Driever W, Fishman MC (1996) Mutations affecting development of zebrafish digestive organs. Development 123: 321-328.

81. Papasani MR, Robinson BD, Hardy RW, Hill RA (2006). Early developmental expression of two insulins in zebrafish (*Danio rerio*). Physiol Genomics 27(1): 79-85.

82. Pauls S, Zacchin E, Tiso N, Bortolussi M, Argenton F (2007) Function and regulation of zebrafish nkx2.2a during development of pancreatic islets and ducts. Dev Biol 304: 875-890.

83. Pelletier G (1977) Identification of four cell types in the human endocrine pancreas by immunoelectron microscopy. Diabetes 26(8): 749-756.

84. Pick A, Clark J, Kubstrup C, Levisetti M, Pugh W, BonnerWeir S, Polonsky KS (1998) Role of apoptosis in failure of beta-cell mass compensation for insulin resistance and beta-cell defects in the male Zucker diabetic fatty rat. Diabetes 47: 358-364.

85. Pictet RL, Clark WR, Williams RH, Rutter WJ (1972) An ultrastructural analysis of the developing embryonic pancreas. Dev Biol 29: 436-467.

86. Pisharath H, Rhee JM, Swanson MA, Leach SD, Parson MJ (2007) Targeted ablation of beta cells in the embryonic zebrafish pancreas using *E. coli* nitroreductase. Mech Dev 124: 218-229.

87. Poncelet DA, Bellefroid EJ, Bastiaens PV, Demoitie MA, Marine JC, Pendeville H, Alami Y, Devos N, Lecocq P, Ogawa T, Muller M, Martial JA (1998)

Functional analysis of ZNF85 KRAB zinc finger protein, a member of the highly homologous ZNF91 family. DNA Cell Biol 17: 931-943.

88. Qiu Y, Sharma A, Stein R (1998) p300 mediates transcriptional stimulation by the basic helix-loop-helix activators of the insulin gene. Mol Cell Biol 18(5): 2957-2964.

89. Rohatgi R, Milenkovic L, Scott MP (2007) Patched1 regulates hedgehog signaling at the primary cilium. Science 317: 372-376.

90. Rosenbaum JL, Witman GB (2002) Intraflagellar transport. Nat Rev Mol Cell Biol 3: 813-825.

91. Rossi JM, Dunn NR, Hogan BL, Zaret KS (2001) Distinct mesodermal signals, including BMPs from the septum transversum mesenchyme, are required in combination for hapatogenesis from the endoderm. Genes Dev 15: 1998-2009.

92. Rukstalis JM, Habener JF (2009) Neurogenin3: a master regulator of pancreatic islet differentiation and regeneration. Islets 1(3): 177-184.

93. Saunier S, Salomon R, Antignac C (2005) Nephronophthisis. Curr Opin Genet Dev 15: 324-331.

94. Senee V, Chelala C, Duchatelet S, Feng D, Blanc H, Cossec JC, Charon C, Nicolino M, Boileau P, Cavener DR, Bougnères P, Taha D, Julier C (2006) Mutations in GLIS3 are responsible for a rare syndrome with neonatal diabetes mellitus and congenital hypothyroidism. Nat Genet 38: 682-687.

95. Sharma A, Stein R (1994) Glucose-induced transcription of the insulin genesis mediated by factors required for β-cell type specific expression. Mol Cell Biol 14: 871-879.

96. Shi S, Cote RJ, Taylor CR (1997) Antigen retrieval immunohistochemistry: past, present, and future. J Histochem Cytochem 45: 327-343.

97. Simmons RA, Templeton LJ, Gertz SJ (2001) Intrauterine growth retardation leads to the development of type 2 diabetes in the rat. Diabetes 50: 2279–2286.

98. Simms D, Cizdziel PE, Chomczynski P (1993) TRIzol: a new reagent for optimal single-step isolation of RNA. Focus 15(4): 99-102.

99. Slack JMW (1995) Developmental biology of the pancreas. Development 121: 1569-1580.

100. Solar M, Cardalda C, Houbracken I, Martín M, Maestro MA, Medts ND, Xu X, Grau V, Heimberg H, Bouwens L, Ferrer J (2009) Pancreatic exocrine duct cells give rise to insulin-producing β cells during embryogenesis but not after birth. Dev Cell 17: 849-860.

101. Spooner BS, Walther BT, Rutter WJ (1970) The development of the dorsal and ventral mammalian pancreas in vivo and in vitro. J Cell Biol 47: 235-246.

102. Stafford D, Prince VE (2002) Retinoic acid signaling is required for a critical early step in zebrafish pancreatic development. Curr Biol 12:1215-1220.

103. Streisinger G, Walker C, Dower N, Knauber D, Singer F (1981) Production of clones of homozygous diploid zebra fish (Brachydanio rerio). Nature 291: 293-296.

104. Swenne I (1982) The role of glucose in the in vitro regulation of cell cycle kinetics and proliferation of fetal pancreatic beta-cells. Diabetes 31: 745-760.

105. Taha D, Barbar M, Kanaan H, Williamson Balfe J (2003) Neonatal diabetes mellitus, congenital hypothyroidism, hepatic fibrosis, polycystic kidneys, and congenital glaucoma: a new autosomal recessive syndrome? Am J Med Genet A 122(A): 269273.

106. Talchai C, Lin HV, Accili D (2009) Genetic and biochemical pathways of B-cell failure in type 2 diabetes. Int Congr Ser 11(4): 38-45.

107. Taniguchi CM, Emanuelli B, Kahn CR (2006) Critical nodes in signaling pathways: insights into insulin action. Nature Rev Mol Cell Biol 7: 85-96.

108. Teta M, Long SY, Wartschow LM, Rankin MM, Kushner JA (2005) Very slow turnover of beta-cells in aged adult mice. Diabets 54:2557-2567.

109. Torres VE, Harris PC (2006). Mechanisms of disease: autosomal dominant and recessive polycystic kidney diseases. Nat Clin Pract Nephrol 2: 40-55.

110. Vargesson NA (2007) Zebrafish. Manual of Animal Technology (ed. S. Barnett) Blackwell Publishing Ltd: Oxford, UK.

111. Veland IR, Awan A, Pedersen LB, Yoder BK, Christensen ST (2009) Primary cilia and signaling pathways in mammalian development, health and disease. Nephron Physiol 111: 39-53.

112. von Hofsten J, Olsson P (2005) Zebrafish sex determination and differentiation: involvement of FTZ-F1 genes. Reprod Biol Endocrinol 3:63.

113. von Wasielewski R, Werner M, Nolte M, Wilkens L, Georgii A (1994) Effects of antigen retrieval by microwave heating in folrmailin-fixed tissue sections on a broad panel of antibodies. Histochemistry 102(3): 165-172.

114. Wandzioch E, Zaret KS (2009) Dynamic signaling network for the specification of embryonic pancreas and liver progenitors. Science 324(5935): 1707-1710.

115. Wang H, Zhou Q, Kesinger JW, Norris C, Valdez C (2007) Heme regulates exocrine peptidase precursor genes in zebrafish. Exp Biol Med 232: 1170-1180.

116. Watanabe N, Hiramatsu K, Miyamoto R, Yasuda K, Suzuki N, Oshima N, Kiyonari H, Shiba D, Nishio S, Mochizuki T, Okoyama T, Maruyama S, Matsuo S, Wakamatsu Y, Hashimoto H (2009). A murine model of neonatal diabetes mellitus in Glis3 deficient mice. FEBS Lett 583: 2108-2113

117. Williams AJ, Khachigian LM, Shows T, Collins T (1995) Isolation and characterization of a novel zinc-finger protein with transcription repressor activity. J Biol Chem 270: 22143-22152.

118. Williams JA (2010) Regulation of acinar cell function in the pancreas. Curr Opin Gastroenterol 26(5): 478-483.

119. Xu YX, Chen L, Wang R, Hou WK, Lin P, Sun L, Sun Y, Dong QY (2008) Mesenchymal stem cell therapy for diabetes through paracrine mechanisms. Med Hypotheses 71: 390-393.

120. Yang Y, Chang BH, Samson SL, Li MV, Chan L. (2009) The Kruppel-like zinc finger protein Glis3 directly and indirectly activates insulin gene transcription. Nucleic Acids Res 37: 2529-2538.

121. Yang W, Dall TM, Halder P, Gallo P, Kowal SL, Hogan PF (2013a) Economic cost of diabetes in the U.S. in 2012. Diabetes Care 36(4): 1033-1046.

122. Yang Y, Chang BH, Chan L (2013b) Sustained expression of the transcription factor GLIS3 is required for normal beta cell function in adults. EMBO Mol Med 5:92-104.

123. Yee NS, Yusuff S, Pack M (2001) Zebrafish pdx1 morphant displays defects in pancreas development and digestive organ chirality, and potentially identifies a multipotent pancreas progenitor cell. Genesis 30: 137-140.

124. Zecchin E, Mavropoulos A, Devos N, Filippi A, Tiso N, Meyer D, Peers B, Bortolussi M, Argenton F (2003) Evolutionarily role of ptf1a in the specification of exocrine pancreatic fates. Dev Biol 268:174-184.

125. Zecchin E, Filippi A, Biemar F, Tiso N, Pauls S, Ellertsdottir E, Gnugge L, Bortolussi M, Driever W, Argenon F (2007) Distinct delta and jagged genes control sequential segregation of pancreatic cell types from precursor pools in zebrafish. Dev Biol 301: 192-204.

126. ZeRuth GT, Yang X, Jetten AM (2011) Modulation of the transactivation function and stability of Krüppel-like zinc finger protein Gli-similar 3 (Glis3) by suppressor of fused. J Biol Chem 286(25): 22077-22089.

127. ZeRuth GT, Takeda Y, Jetten AM (2013) The Krüppel-like protein Gli-similar 3 (Glis3) functions as a key regulator of insulin transcription. Mol Endocrinol 27(10): 1692-1705.

128. ZeRuth GT, Williams JG, Cole YC, Jetten AM (2015) HECT E3 ubiquitin ligase Itch functions as a novel negative regulator of Gli-Similar 3 (Glis3) transcriptional activity. PLoS ONE 10(7): e0131303.

129. Zhang F, Nakanishi G, Kurebayashi S, Yoshino K, Perantoni A, Kim YS, Jetten AM (2002) Characterization of Glis2, a novel gene encoding a Gli-related, Kruppel-like transcription factor with transactivation and repressor functions, roles in kidney development and neurogenesis. J Biol Chem 277: 10139-10149.

130. Zhou Q, Law AC, Rajagopal J, Anderson WJ, Gray PA, Melton DA (2007) A multipotent progenitor domain guides pancreatic organogenesis. Dev Cell 13: 103-114.

Appendix

Recipes:

Embryo Media 0.5x E2

For 1.0 L

100x E2A	5 ml
500x E2B	1 ml
500x E2C	1 ml
0.1% w/v Methylene Blue	500 ul

Add reverse osmosis (RO) water to 900 ml. Adjust pH to 7.0-7.2 with concentrated HCl or NaOH. Add RO water to 1 L. Store at RT.

100x E2A

For 160 ml

NaCl	14 g
KCl	0.6 g
$MgSO_4$	1.92 g
KH_2PO_4	0.33 g
Na_2HPO_4	0.11 g

Add Millipore water to a final volume of 160 ml. Stir to dissolve reagents. Sterilize by autoclaving. Stir overnight to dissolve any precipitation, store at 4^oC.

500x E2B

<u>For 200 ml</u>

CaCl$_2$ 11 g

Add Millipore water to a final volume of 200 ml. Stir to dissolve reagents. Sterilize by

autoclaving. Aliquot in 20 ml portions. Store at -20°C.

500x E2C

<u>For 200 ml</u>

NaHCO$_3$ 6 g

Add Millipore water to a final volume of 200 ml. Stir to dissolve reagents. Sterilize by

autoclaving. Aliquot in 20 ml portions. Store at -20°C.

Luria Bertani (LB) Media

<u>For 500 ml</u>

Tryptone   5 g

Yeast Extract   2.5 g

NaCl   5 g

Agar (if for plates)   7.5 g

Mix ingredients in 300 ml of water by stirring. Sterilize by autoclaving. Cool to ~55°C

before adding antibiotic.

S.O.C Media

For 100 ml

Tryptone	2 g
Yeast extract	0.5 g
NaCl	200 ul (5 M)
KCl	250 ul (1 M)
$MgCl_2$	1 ml (1 M)
$MgSO_4$	1 ml (1 M)
D-Glucose	2 ml (1 M)

Dissolve first 4 ingredients in 96 ml ddH_2O. Sterilize by autoclaving. Allow to cool to RT. Add last 3 ingredients by syringe filtration. Store at 4° C.

8% Paraformaldehyde

For 100 ml

Paraformaldehyde	8 g
NaOH	600 ul (10 M)

Mix ingredients in 90 ml of water and stir until paraformaldehyde goes into solution without heating. After obtaining a clear solution, add 1 ml 6M HCl and adjust pH to 7.0. To prepare a working solution of 4% PFA, combine 50 ml 8% PFA, 10 ml of 10x PBS, and 40 ml DEPC water.

10x Phosphate Buffered Saline (PBS)

For 500 ml

NaCl   40 g

KCl   1 g

Na_2HPO_4 7.2 g

KH_2PO_4 1.2 g

Disolve reagents in 4oo ml of ddH_2O. Adjust pH to 7.4 with HCl. q.s. to 500 ml with

ddH_2O. Sterilize by autoclaving. Store at RT.

Trypsin Solution (0.05%)

For 10 ml

Trypsin   0.05 g

$CaCl_2$ 0.1 g

Dissolve 0.05 g of trypsin in 10 ml of distilled water. Dissolve 0.1 g of $CaCl_2$ in a

separate container of 10 ml of distilled water. Add 1 ml of the trypsin solution and 1 ml

of the $CaCl_2$ solution to 8 ml of distilled water. Adjsut pH to 7.8 with 1 M NaOH and

store at 4° C.

10x Tris Buffered Saline (TBS)

For 500 ml

Tris   12.1 g

NaCl   48.8 g

Dissolve salts in 400 ml of ddH$_2$O. Adjust pH to 7.6 with HCl. q.s. to 500 ml with ddH$_2$O. Sterilize by autoclaving. Store at RT.

Protocols:

HotSHOT DNA Extraction

1. Immerse tissue in 100 ul of 50 mM NaOH in a 1.5 ml microcentrifuge tube.

    a. Poke a hole in the lid of the microcentrifuge tube.

2. Heat for 20 minutes at 95°C.

    a. Shake tube after heating to dissociate tissue.

3. Chill tubes to 4°C on ice, then add 10 ul of 1 M Tris HCl pH 8.0.

4. Centrifuge for 10 minutes at 4°C at max speed.

    a. DNA is in the supernatant after centrifuging.

5. Determine DNA concentration using a nanodrop.

TOPO TA Cloning

1. Equilibrate a water bath to 42° C.

2. Warm SOC broth and AMP$^+$ LB culture plates to 37° C in an incubator.

3. Set up the TOPO cloning reaction:

    a. 2 ul of PCR product DNA

    b. 1 ul TOPO salt solution

    c. 1 ul TOPO vector

    d. 2 ul RNAse free water

4. Incubate at RT for 5 minutes

5. Add 2 ul of the TOPO cloning reaction to 50 ul of DH5α cells, mix gently.

6. Incubate on ice for 5 minutes.

7. Heat shock in the 42° C water bath for 30 seconds without shaking.

8. Place on ice, and add 250 ul of prewarmed SOC.

9. Shake tubes horizontally for 1 hour at 37° C.

10. Add 50 ul of the transformation to the prewarmed Amp$^+$ LB plate and incubate overnight at 37° C.

11. Choose 3 to 4 colonies and incubate each in 3 ml of AMP$^+$ LB broth at 37° C while rocking horizontally.

12. Purify amplified DNA using a plasmid miniprep kit.

Site Directed Mutagenesis

1. Dilute plasmid DNA (from TOPO TA cloning) to 50 ng/ul.

2. Set up PCR reaction:

   a. 5 ul of 10x PFU buffer.

   b. 1.25 ul of 100 ng/ul forward primer.

   c. 1.25 ul of 100 ng/ul reverse primer.

   d. 1 ul of dNTP mix.

   e. 1 ul of 50 ng/ul plasmid DNA

   f. RNAse free water to a final volume of 50 ul.

3. Add 1 ul of PFU Turbo DNA polymerase

4. Run PCR cycle:

   a. 1 cycle

      i. 95° C for 30 seconds.

   b. 12 cycles

        i.   95º C for 30 seconds.

        ii.   55º C for 1 minute.

        iii.   68º C for 5 minutes.

   c. 1 cycle

        i.   68º C for 10 minutes.

5. Add 1 ul of Dpn I restriction enzyme.

6. Gently mix the reaction, then spin down for one minute.

7. Incubate at 37º C for 1 hour.

8. Add 45 ul of XL10-Gold competent cells and 2 ul of β-mercaptoethanol to a separate, prechilled microcentrifuge tube.

   a. Incubate on ice for 10 minutes, swirling every 2 minutes.

9. Add 2 ul of Dpn I treated DNA to the tube and incubate on ice for 30 minutes.

10. Transfect mutated DNA into the XL10-Gold competent cells (Steps 7-12 from TOPO TA Cloning protocol).

TaqMan SNP Genotyping Assay

1. Create a master mix using, for each sample:

   a. 12.5 ul of 2x TaqMan Universal PCR Master Mix.

   b. 1.25 ul of 20x SNP Genotyping Assay

   c. 9.25 ul of RNAse free water.

2. Load the master mix into an RT-PCR well plate. Each sample gets 23 ul of the master mix and 2 ul 25 ng/ul DNA.

3. Run the PCR cycle

   a. 1 cycle

       i. 95° C for 10 minutes.

  b. 40 cycles

       i. 92° C for 15 seconds.

      ii. 60° C for 1 minute.

TRIzol RNA Extraction

1. Place ~30 eggs (or organ tissue) in a 1.5 ml sterile microcentrifuge tube.

2. Add 250 ul of TRIzol and lyse cells with a pestle.

3. Add 750 ul of TRIzol and incubate at RT for 5 minutes.

4. Add 200 ul of phenol:chloroform and gently invert for 15 seconds.

5. Incubate at RT for 2 minutes, then centrifuge at 12,000 x g for 15 minutes at 4° C.

6. Transfer the clear aqueous top layer to a new tube and add 500 ul of isopropanol.

7. Incubate at RT for 10 minutes.

8. Spin for 10 minutes at 12,000 x g and 4° C. Remove supernatant and wash in 1 ml of 75% ethanol.

9. Centrifuge for 5 minutes at 7,500 x g and 4° C. Remove ethanol and allow pellet to air dry for 10 minutes while inverted.

10. Resuspend RNA in 100 ul of RNAse free water, store at -80° C.